BORATE MINERALS FROM THE KRAMER DISTRICT, MOHAVE DESERT, CALIFORNIA

By WALDEMAR T. SCHALLER

SUMMARY

The development of the borate deposits of the Kramer district, in the Mohave Desert, Calif., received a strong impulse in 1926 by the discovery there of a large deposit of the new sodium borate, kernite. This deposit lies about 2½ miles east of the original discovery of colemanite and ulexite in the Suckow shaft. All the borates occur underground, there being no indication whatever at the surface of the existence of any borates below. The original discovery was made in drilling for water.

The first sample of these borate minerals was received by the writer from Hoyt S. Gale, of Los Angeles, in the fall of 1926. In September, 1927, through the courtesy of Mr. Clarence M. Rasor, of the Pacific Coast Borax Co., an opportunity was had to visit the kernite deposit and collect material, which forms the basis of this report. The kindness of Mr. Rasor in allowing the collection and study of material is much appreciated.

The geologic setting of the kernite deposit is imperfectly known, but in general it is similar to that of the deposits a few miles west which have been described by Noble. The borate minerals, several hundred feet underground, occur in a complex clay series and are underlain by igneous rock, whether extrusive (and therefore of earlier age than the borates) or intrusive (and therefore of later age than the borates) is not known. Knowledge of this relative age of the lava would be of great help in understanding the genesis of the borate minerals.

The borate minerals found include colemanite, ulexite, borax, tincalconite, and two new borates, kernite and kramerite. The associated minerals are calcite, realgar, stibnite, and the clay minerals. Kernite was briefly described in a preliminary paper in January, 1927; kramerite is first described in this paper. Abundant and better material, recently collected by the writer, has furnished the basis for fuller description of kernite and also shows that some of the statements made in the original brief paper need to be corrected.

The composition of the two new minerals is as follows:

Kernite, $Na_2O.2B_2O_3.4H_2O$.

Kramerite, $Na_2O.2CaO.5B_2O_3.10H_2O$.

Kernite occurs in greater quantity and is of greater interest scientifically. It is the commercial mineral mined, existing as an immense deposit a hundred feet thick and many hundred feet in lateral extent. The deposit contains an estimated minimum of well over a million tons. Some of the crystals are of immense size, the largest one seen measuring 8 feet in thickness. Many of the crystals are several feet across. The mineral belongs chemically to the borax group but has only 4 molecules of water instead of 10, as in borax. The crystals are monoclinic, with the axial ratio $a : b : c = 1.5230 : 1 : 1.6989$, $\beta = 71° 08'$. Thirty-six crystal forms were observed, together with many additional vicinal forms. Two perfect cleavages break the mineral up into elongated rhombic prisms.

Kramerite occurs in small quantities as radiating prisms, averaging not over a millimeter in thickness. It is monoclinic, with the axial ratio $a : b : c = 1.1051 : 1 : 0.5237$, $\beta = 72° 16'$. Eight crystal forms were identified. In composition, kramerite is like ulexite but with less water. It was probably artificially made by Van't Hoff. The prisms of kramerite cut the clay, kernite, and borax and are of later origin.

Tincalconite, $Na_2O.2B_2O_3.5H_2O$, named by Shephard in 1878, is, as found, always secondary, forming by dehydration of borax and by hydration of kernite. It is a finely crystalline aggregate, existing only as a coating on the other borates.

These three sodium borates have been made artificially in the chemical laboratory of the Geological Survey in Washington. A comparison of the properties of a number of hydrates in the different series—the borax series, the colemanite series—has been made.

The origin of the deposit forms a separate problem in which the mineral relationships are the chief criteria. The geologic relations are so little known in detail that the processes of formation can only be suggested at this time. The kernite was perhaps formed by the fusion in its own water of crystallization of a previous accumulation of borax crystals, enough water being driven off to yield on solidification of the fused borax the 4-hydrate kernite. If no water could escape the resultant product was massive borax.

A list of all known boron minerals is added, with some critical remarks about their relationship and standing. A bibliography of the borate minerals of the Kramer district ends the paper.

LOCALITY

The Kramer borate district lies in southeastern Kern County, Calif., only a few miles west of the San Bernardino County line. The deposits of borate minerals are about 7 miles northwest of Kramer and 28 miles due east of Mojave. The first borate discovery was made in sec. 22, T. 11 N., R. 8 W., where, in 1913, colemanite and ulexite were found. The kernite deposit, first actively opened in 1926, lies on the boundary between sec. 24, T. 11 N., R. 8 W., and sec. 19, T. 11 N., R. 7 W. The deposits are only a few miles north of the main line of the Atchison, Topeka & Santa Fe Railway.

GEOLOGIC SETTING

The deposit of colemanite and ulexite in the western part of the Kramer borate district has been described by Noble [1] and Gale.[2]

The borate deposits lie in tilted and faulted beds of clay shale at least 100 feet beneath one of the gently sloping alluvial plains that form so characteristic a

[1] Noble, L. F., Borate deposits in the Kramer district, Kern County, Calif.: U. S. Geol. Survey Bull. 785, pp. 45–61, 1926.

[2] Gale, H. S., Borate deposits near Kramer, Calif.: Am. Inst. Min. and Met. Eng. Trans., vol. 73, pp. 449–463, 1926.

feature of the desert region. This alluvial plain of sand and gravel is bordered on the northeast by low hills of lava and tuff. A bed of basaltic lava underlies the borate deposits. The clay shale and the lava are of Tertiary age.

According to Noble, a bed of arkose sandstone overlies the borate-bearing shale in the Suckow shaft No. 2, 2½ miles west of the kernite deposit, where colemanite and ulexite are the only borate minerals present. The clay material containing lenses and nodules of colemanite, irregularly distributed, differs from the clay deposited upon the surface of Rogers Lake and other playas in the desert at the present time only in that it has been consolidated into shale, tilted, eroded, and buried. The clay matrix of the kernite deposit is more complex and is composed of a diverse set of materials. Noble considers the deposit in the region of the Suckow shaft to have been originally a playa deposit, the borate mineral ulexite forming in the mud of the drying lake and the colemanite being formed later by alteration of the ulexite, as postulated by Foshag.[3]

The bed of basaltic lava underlying the borate deposits is believed by Noble to have been poured out just before the shale was deposited and to be, indirectly, the source of the boron, which was derived from the hot springs and solfataras connected with the volcanic activity. A bed of igneous rock is likewise reported to underlie the kernite deposit.

According to the records, although the igneous rock beneath the borates was found wherever the borings were deep enough, the borate minerals were not encountered everywhere. They are extremely irregular in form and distribution, the structure of their Tertiary host rocks is exceedingly complex, and "the limits of the deposits can be determined only by underground exploration."[4] The report by Noble was written before the kernite deposit was discovered. The relations of the clay shale and the igneous rock to the kernite deposit are discussed under the heading "Origin of deposit."

The borate minerals known to occur in the Kramer district are as follows: Colemanite and ulexite, probably the most widespread, have been found wherever any borates occur. They are the minerals reported from the original discovery. Apparently they are the only borates found in any of the shafts and borings in sec. 22. At the kernite deposit, colemanite and ulexite occur in the clay above the kernite. Associated with the kernite are borax, tincalconite, and kramerite. Other minerals associated with these borates are the clay minerals, the rock minerals (feldspars, micas, etc.) found in the clay, calcite, stibnite, and realgar.

[3] Foshag, W. F., The origin of the colemanite deposits of California: Econ. Geology, vol. 16, p. 210, 1921.

[4] Noble, L. F., op. cit., p. 51.

BORATE MINERALS

COLEMANITE

The colemanite from the Kramer district yields good examples illustrating its derivation from ulexite, especially as small spherical masses of radiating crystals are embedded in ulexite and evidently derived therefrom, as indicated by Foshag. A specimen obtained above the kernite deposit, kindly presented by Mr. Rasor for study, shows the development of a group of compacted crystals of colemanite, as much as an inch thick, growing in the ulexite. This specimen is shown in Plate 22, *B*.

A number of specimens collected from one of the dumps in sec. 22 show clearly the nodular colemanite formed from ulexite, with a very small quantity of the ulexite still remaining. The centers of the nodules consist of compact colemanite in which are scattered bands of residual ulexite fibers. Around the massive center radiating bunches of colemanite fibers and plates have grown. Both the fibrous and the massive variety have the optical properties of colemanite, as the following tabulation shows:

Optical properties of colemanite

	As given by Larsen	Massive variety	Fibrous variety
α	1. 586	1. 586	1. 585
β	1. 592	1. 591	1. 590
γ	1. 614	1. 613	1. 614
Sign	+	+	+
$Z \wedge c$	6°	Very small.	5°
2E	97°	Large.	Large.

Most of the fibers have positive, though a few have negative elongation.

Colemanite does not seem to be very abundant in the eastern part of the field, where the kernite occurs. Only a few specimens, all associated with ulexite, were seen in the clay above the kernite.

ULEXITE

Ulexite occurs abundantly as compact fibrous veins in the clay shale. The familiar "cotton-ball" variety was not observed. Noble describes the ulexite found in sec. 22 as "compact." That occurring above the kernite is in beautiful veins of pure white material, affording a fine example of "satin spar." These veins may be several inches in thickness. Such an example, with crystals of colemanite developed in the ulexite, is shown in Plate 22, *B*. A set of smaller veins, with a beautiful "satin spar" luster, is shown in Plate 22, *A*. The relative position of these two specimens is not known, but they probably came from slightly different horizons, as the clay matrix shows considerable difference. But both are from the clay above the kernite.

A similar compact ulexite was reported from Lang, 55 miles to the southwest, by Foshag,[5] who states:

[5] Foshag, W. F., op. cit., p. 204.

It is not the ordinary "cotton-ball" type but is massive and fibrous. It has the appearance of cotton balls that have been consolidated by pressure. The ulexite occurs in irregular masses, more or less lenslike and surrounded by thin layers of clay. In structure these lenses are compact-fibrous, the fibers oriented in all directions in the centers and parallel at the peripheries.

Similar masses of ulexite are to be found in the Kramer district, but veins which have a straight parallel fiber structure, such as is shown in Plate 22, *A*, and which occur above the kernite probably did not form by the consolidation of "cotton balls" without going into solution and being redeposited. A curious growth of masses of ulexite, resembling in form a cone-shaped fungus, was also encountered. The shaft through the clay containing the ulexite, above the kernite, was boarded up at the time of examination, so that the relation of the ulexite-bearing clay to the kernite-bearing clay is unknown.

Examined in crushed fragments, the ulexite is seen to be intimately polysynthetically twinned, the traces of the twinning plane being parallel with the elongation of the fibers, which is generally negative, though a few fibers with a positive elongation were noticed. Y is approximately parallel with the elongation. The optical properties are the same as those of normal ("cotton-ball") ulexite.

Optical properties of ulexite

	As given by Larsen	Satiny ulexite
α	1. 491	1. 493
β	1. 504	1. 506
γ	1. 520	1. 519
Sign	+	+
$Y \wedge c$	0° to 23°	Variable, about 20°
2V	Moderate to large.	Large.

The density of this fibrous ulexite was determined to be 1.963.

The fine satiny ulexite shown in Plate 22, *A*, has the normal chemical composition, as shown by the following analyses:

Analyses of satin spar variety of compact ulexite.

	1	2	3
CaO	14. 06	14. 14	13. 85
Na_2O	7. 09	[a] 7. 06	7. 65
B_2O_3	42. 94	43. 12	42. 95
H_2O	35. 54	35. 68	35. 55
Insoluble	. 10		
	99. 73	100. 00	100. 00

[a] By difference.

1. Analyst, W. T. Schaller; Kramer district, Calif.
2. Analyst, W. F. Foshag; Lang, Calif.
3. Calculated.

The analyses represent the figures for the established formula of ulexite, $Na_2O.2CaO.5B_2O_3.16H_2O$. By heating this ulexite, in a powdered form, in a sealed tube with a saturated solution of sodium chloride in the steam bath for a week, it was readily changed to the lower hydrate, kramerite, as described under the synthesis of that mineral.

KRAMERITE

CHARACTER OF MATERIAL

Groups of spherulites were noted as rather abundant near the floor of one of the drifts in the kernite mine. They proved to be a new mineral, a hydrous sodium-calcium borate, $Na_2O.2CaO.5B_2O_3.10H_2O$, of the same type of formula as ulexite ($Na_2O.2CaO.5B_2O_3.16H_2O$) but with less water. The name kramerite is given to this mineral, after the name of the district, which evidently was so named after Kramer, the nearest town.

Kramerite is in prismatic crystals, usually forming spherulites but also more rarely existing as single crystals or groups of prisms in more or less parallel position, or in radiating groups that do not form a complete spherulite. The diameter of the spherulites averages from 3 to 4 centimeters. The center is usually composed only of kramerite, but there is no sharp outer boundary, the prismatic crystals, in places considerably bent, projecting into the matrix for unequal distances. The longest individual crystal measured extended for 23 millimeters (about an inch), although still longer ones probably occur. The crystals are approximately a quarter to half a millimeter in average thickness.

The crystals penetrate indifferently both the clay matrix and the associated massive borax and highly cleavable kernite and seem to be the next to the last borate mineral of the deposit to form, tincalconite being the last. Although the striking spherulites were noticed at only one place in the mine, extending over a distance of but a few feet, crystals of kramerite probably are widely distributed throughout the deposit, for a few individual prisms or small radiating groups were noticed on many of the other specimens collected. The typical appearance is shown in Plate 23. The minute black spherulites of stibnite, a little calcite, and the clay are the only boron-free mineral associates noted. In the laboratory the borax of the specimens readily dehydrates to tincalconite in which the bright prisms of kramerite stand out, this mineral retaining its glassy luster and not becoming dull and white. On the specimens where the borax has become partly dehydrated, the center portion of the kramerite spherulites appears considerably darker against the dull-white background.

PHYSICAL AND OPTICAL PROPERTIES

Kramerite is colorless and transparent. It has a perfect prismatic cleavage, parallel to *m* (110), a hardness of about 2½, and a density of 2.141. The luster is vitreous, and the crystals remain bright and shining.

The mineral is monoclinic prismatic. The optic axial plane is parallel to the clinopinacoid b (010), Y $= b$ axis, Z $\wedge$ c axis $= 12°$. Crystals lying on a (100), with parallel extinction, show part of one optic eye of the obtuse figure. Parallel to m (110), the extinction is about 14°. The sign is positive, and the axial angle is large. 2V (measured) 73°, 2E 126°. Dispersion $\rho > v$. The elongation of the crystals is positive.

The optical orientation of kramerite is shown in Figure 19. The refractive indices are $\alpha = 1.515$, $\beta = 1.525$, $\gamma = 1.544$. C. S. Ross obtained α 1.514, $\beta = 1.524$, $\gamma = 1.543$. The birefringence is 0.029, and crushed fragments show brilliant colors. Kramerite is commonly not twinned, and the absence of twinning lamellae, so characteristic of ulexite, serves as an immediate criterion for its differentiation. An examination of crushed fragments, however, occasionally shows what might be simple twinning.

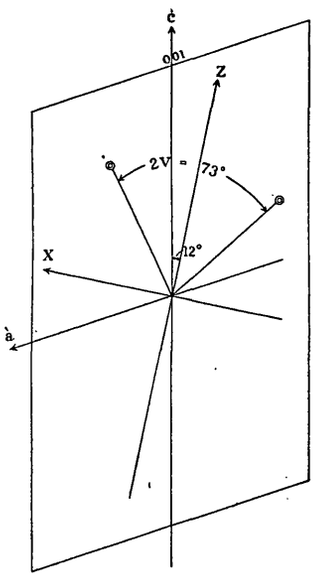

FIGURE 19.—Optical orientation of kramerite

CRYSTALLOGRAPHY

GENERAL DESCRIPTION

The prismatic monoclinic crystals are simple in their combinations and show all the unit forms except the base. Fourteen crystals were measured, but many more were examined under the microscope. No twins were seen. The crystals are all long prismatic in habit.

The forms present are

a (100)	m (110)	t (101)	p (111)
b (010)	e (011)	d ($\bar{1}$01)	o ($\bar{1}$11)

CALCULATION OF ELEMENTS

The axial ratios are $a : b : c = 1.1051 : 1 : 0.5237$, $\beta = 72° 16'$, $p'_0 = 0.4976$, $q'_0 = c = 0.5237$, $e' = 0.3197$. These elements were derived from the average measurements (ϕ and ρ) of m (110) and e (011). For m (110), the ϕ readings averaged 43° 32′, as follows:

Average of 24 most consistent readings, ranging from 43° 26′ to 43° 41′	43° 33′
Average value, on four crystals, where all four faces of m were measured accurately	43° 31½
Average for crystal 11 (readings 43° 31′, 43° 32′, 43° 31′, 43° 32′, all good)	43° 31½
Average ϕ	43° 32′

The total readings on m (110), exclusive of those due to the vicinal faces and those where the striations permitted only an approximate centering of the reflections, for 38 readings, ranging from 43° 03′ to 43° 56′, averaged 43° 29′.

The average of the 12 best measurements of good and fair reflections of the clinodome e (011) gave:

ϕ (from 31° 01′ to 31° 51′), 31° 24′
ρ (from 31° 26′ to 31° 36′), 31° 32′

From these average values—namely, ϕ (110) $= 43° 32'$, ϕ (011) $= 31° 24'$, and ρ (011) $= 31° 32'$—the axial elements as given are calculated.

FORMS AND ANGLES

The measured and calculated angles for all the forms are as follows:

Measured and calculated angles of kramerite

Form	Measured		Calculated	
	ϕ	ρ	ϕ	ρ
	° ′	° ′	° ′	° ′
a (100)	90 00	90 00	90 00	90 00
b (010)	0 03	90 00	0 00	90 00
m (110)	43 32	90 00	43 32	90 00
t (101)	90 02	39 13	90 00	39 16
d ($\bar{1}$01)	89 56	9 53	90 00	10 05
e (011)	31 24	31 32	31 24	31 32
p (111)	57 12	44 08	57 21	44 09
o ($\bar{1}$11)	20 00	30 06	18 45	28 57

The individual measurements of the different forms are as follows, those measurements which, owing chiefly to striations, served only to identify the forms being omitted.

Measurements of a (100), kramerite

Crystal No.	Size	Reflection	Measured ϕ (calculated, 90° 00′)
			° ′
1	Medium	Fair	89 53
1	do	Poor	91 16
2	do	Good	89 56
2	Small	Poor	90 08
3	do	do	
4	Large	do	88 50
4	do	do	89 29
5	Medium	Good	90 52
5	do	do	89 09
6	Large	do	90 00
6	do	Poor	
7	Medium	do	90 11
8	Large	do	90 31
8	Medium	do	90 02
9	do	Fair	89 59
10	Large	Good	90 02
10	do	do	90 12
11	Medium	do	90 12
12	Large	Fair	89 08
12	Medium	Poor	90 27
13	Large	Fair	90 00
14	Small	Good	89 48

Measurements of b (010), kramerite

Crystal No.	Size	Reflection	Measured ϕ (calculated, 0° 00′)
			° ′
1	Line face	Poor	[a] 0 07
1	do	do	
2	do	do	03
3	do	do	12
4	do	do	11
4	do	do	01
5	do	do	
5	Small	Fair	19
6	Line face	Poor	
6	do	do	49
7	do	do	
8	do	do	15
9	Small	Good	02
9	do	Poor	10
10	Line face	do	20
10	Small	do	01
12	do	do	02
13	do	do	
14	do	Fair	10
14	Line face	Poor	

[a] The positive or negative character of the deviation in angle from 0° 00′ is not indicated.

Measurements of m (110) and accompanying or replacing vicinal form, kramerite

Crystal No.	Size	Reflection	Measured ϕ (calculated, 43° 32′)		Vicinal form	
			°	′	°	′
1	Medium	Good	43	26		
1	do	do	43	37	38	17
1	Line face	Poor	43	11		
2	Medium	Fair	43	29		
2	Line face	Poor				
2	Medium	Good	43	56		
2	do	Poor	43	46		
3	do	Fair	43	37		
3	Small	Poor	43	16		
3	Medium	do	43	56		
3	Small	do				
4	Medium	do	42	44	40	18
4	do	do	41	44	41	06
4	do	do	43	05	40	32
4	do	Fair	43	32		
5	do	Good	43	12		
5	Small	Fair	43	39		
5	Medium	do	42	23		
5	Small	Poor			38	43
6	Medium	Good	43	31		
6	do	Fair	43	19		
6	do	Good	43	33		
6	Small	Poor	43	38		
7	Medium	do				
8	do	do			41	48
8	do	do			41	16
8	do	Good	43	32		
8	Small	Poor	43	12		
9	do	do			38	37
9	do	do			41	14
9	do	do	43	33		
9	Medium	Good	43	18		
10	Line face	Poor			39	23
10	do	do			39	13
10	Small	Fair	43	29		
10	do	Poor	43	26		
11	Medium	Fair	43	32	41	38
11	do	Good	43	31		
11	do	do	43	32		
11	do	do	43	31		
12	do	Fair	43	41		
12	do	Poor	43	37		
12	do	Fair	43	29		
12	do	do	43	33		
13	do	do	43	35	40	58

Measurements of m (110) and accompanying or replacing vicinal form, kramerite—Continued

Crystal No.	Size	Reflection	Measured ϕ (calculated, 43° 32′)		Vicinal form	
			°	′	°	′
13	Medium	Fair	43	32		
13	do	do	43	09		
13	do	do	43	36	39	38
14	Large	do	43	03		
14	Medium	Good	43	13	41	05
14	do	Fair	43	45		

Accompanying the reflection for *m* (110), especially if the face was striated and thereby somewhat rounded, there was, on many crystals, a distinct second signal, close to the one from *m* (110), which gave inconsistent readings ranging from 38° 17′ to 41° 48′. For eight of the fifteen occurrences of the vicinal prism, it accompanied the face of *m* (110); for the remaining seven occurrences it replaced *m* (110). On crystals Nos. 8, 9, and 10, where on each one there were two faces of *m* (110) and two faces of the vicinal form, each pair of faces was grouped around *b* (010). The vicinal form was always striated; if the prism face was not striated and gave a single distinct reflection its measurement was that of *m* (110).

Measurements of e (011), kramerite

Crystal No.	Size	Reflection	Measured ϕ (calculated, 31° 24′)		Measured ρ (calculated, 31° 32′)	
			°	′	°	′
1	Medium	Poor	32	08	31	45
1	Small	do	31	51	31	28
2	do	do	30	48	31	23
4	Large	Fair	31	49	31	36
4	do	do	31	43	31	36
5	do	do	31	51	31	29
5	Medium	do	31	10	31	34
6	Large	Good	31	19	31	30
6	do	do	31	34	31	32
7	Small	Fair	31	15	31	32
8	Large	do	31	30	31	26
8	do	do	31	25	31	26
9	do	Good	31	01	31	34
9	Small	Fair	31	01	31	34
10	Medium	Poor	31	50	31	36
10	Small	do	32	21	31	36
11	Large	Fair	31	12	31	36

Measurements of t (101), kramerite

Crystal No.	Size	Reflection	Measured ϕ (calculated, 90° 00′)		Measured ρ (calculated, 39° 16′)	
			°	′	°	′
1	Line face	Poor	89	47	39	00
2	Small	do	90	12	38	51
4	Large	Fair	90	19	39	16
5	Medium	Poor	89	09	39	30
7	Line face	None[a]	90	11	40	15
8	Large	Fair	90	14	39	07
9	do	do	90	00	39	19
11	Small	Poor	90	11	39	13
12	Line face	None				
13	Small	Poor	90	13	39	29

[a] Where no reflection of the signal was obtained, the measurements were made by maximum brightness.

Measurements of d ($\bar{1}01$), kramerite

Crystal No.	Size	Reflection	Measured ϕ (calculated, 90° 00′)	Measured ρ (calculated, 10° 05′)
			° ′	° ′
3	Small	Poor	89 18	10 04
5	do	do	92 20	9 14
6	Minute	None	90 01	11 20
7	do	do	90 11	9 22
11	do	do	89 55	10 04
13	do	do	90 13	9 11

Measurements of o ($\bar{1}\bar{1}1$), kramerite

Crystal No.	Size	Reflection	Measured ϕ (calculated, 18° 45′)	Measured ρ (calculated, 28° 57′)
			° ′	° ′
2	Line face	Poor	21 26	28 44
3	Minute	do	19 12	31 12
3	do	do	18 25	27 47
11	do	do	21 55	31 35
14	do	do	19 03	31 12

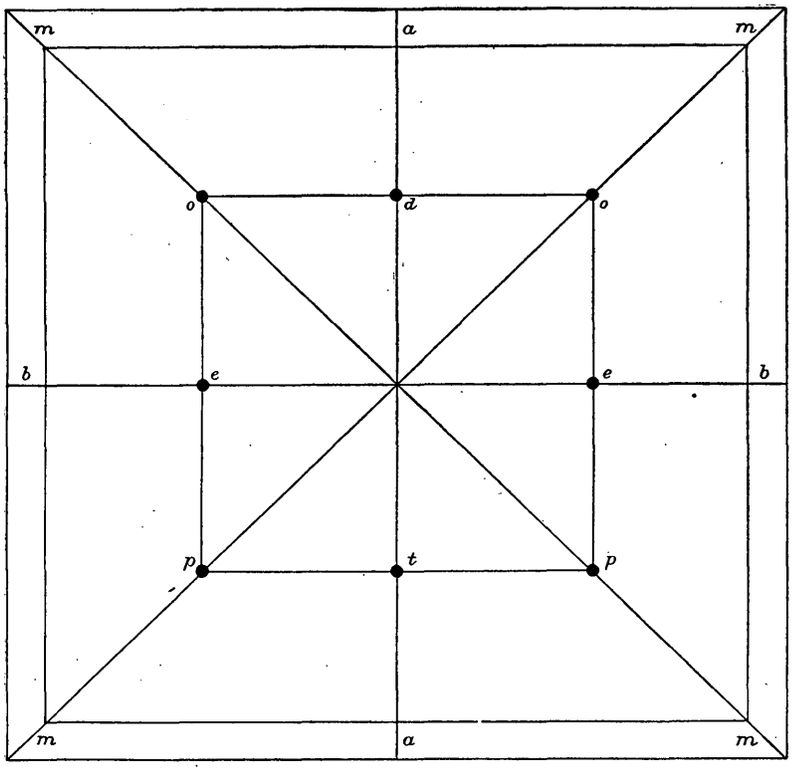

FIGURE 20.—Gnomonic projection of kramerite forms

Measurements of p (111), kramerite

Crystal No.	Size	Reflection	Measured ϕ (calculated, 57° 21′)	Measured ρ (calculated, 44° 09′)
			° ′	° ′
1	Medium	Poor	56 30	44 31
2	Small	do	56 46	43 54
2	Minute	do	57 28	43 42
3	Large	Fair	57 12	44 06
3	Minute	Poor	57 47	44 06
5	Large	Fair	57 35	44 11
5	Minute	Poor	56 42	44 29
7	Small	do	57 39	44 09
7	do	do	56 58	44 06
10	Medium	do	56 24	44 37
11	Large	Fair	57 20	43 56
11	do	Poor	57 36	44 08
12	do	Fair	57 26	44 18
12	do	Poor	57 37	43 55
13	Medium	do	56 35	44 10
14	Large	Fair	57 35	43 57

The gnomonic projection of the crystal forms of kramerite is shown in Figure 20. The projection has a striking isometric symmetry; this pseudoisometric symmetry is brought out still more clearly if in the axial ratios, as given, the c axis is doubled, or still better if the values for p_o' and q_o' are doubled. The pseudoisometric ratio of the crystallographic axes may then be written:

$$a : b : 2c = 1.1051 : 1 : 1.0474$$
$$2p_o' = 0.9052,\ 2q_o' = 1.0474$$

DESCRIPTION OF FORMS

The orthopinacoid a (100) is the largest form on the crystals of kramerite. On most crystals it is larger than the prism faces, though on a few it is of about the same size. Only rarely is it smaller than the prisms, occasionally being only a broad line face. On crystal 14, Figure 23, only one narrow face of a (100) is present. It is generally striated vertically and may be sufficiently rounded to give a row of reflections many degrees apart. The two faces of the form are not of equal size on all crystals. It is, however, the universal and dominant form on nearly all the crystals. When it and the prism faces are nearly of the same size, the crystal has a six-sided cross section (figs. 21, 22, 25, 26); when the faces are large, the crystal is flattened parallel to it (fig. 24).

The clinopinacoid b (010) is a very narrow face, only rarely becoming nearly as large as the prisms. It is striated vertically and, if broader than a line face, is rounded over a considerable angle. A few crystals suggest that an imperfect cleavage may exist parallel to this form. It is present on all but one (No. 11) of the crystals measured. Reexamination of this crystal failed to show any face of this form.

The prism m (110) is universally present and is the second largest form. With the orthopinacoid it determines the habit of the crystals. Many of the faces give good single reflections; on some crystals the unit prism is accompanied by or replaced by a vicinal form, but a few degrees off, lying between it and b (010).

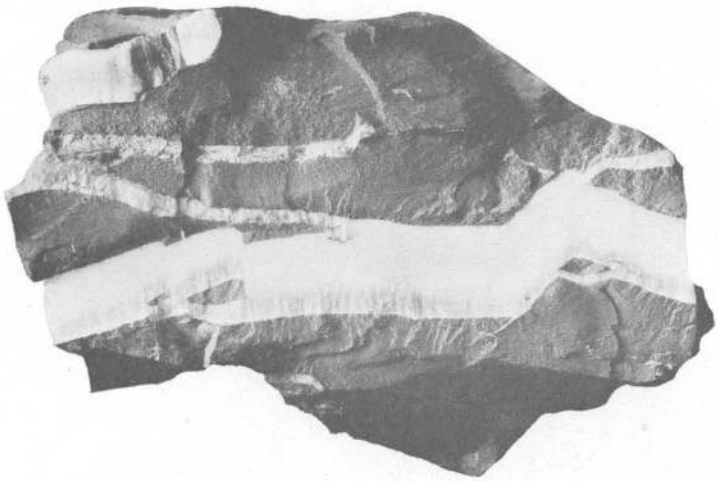

A. SEAMS OF ULEXITE IN CLAY ABOVE KERNITE DEPOSIT

U. S. National Museum catalog No. 95831. Natural size.

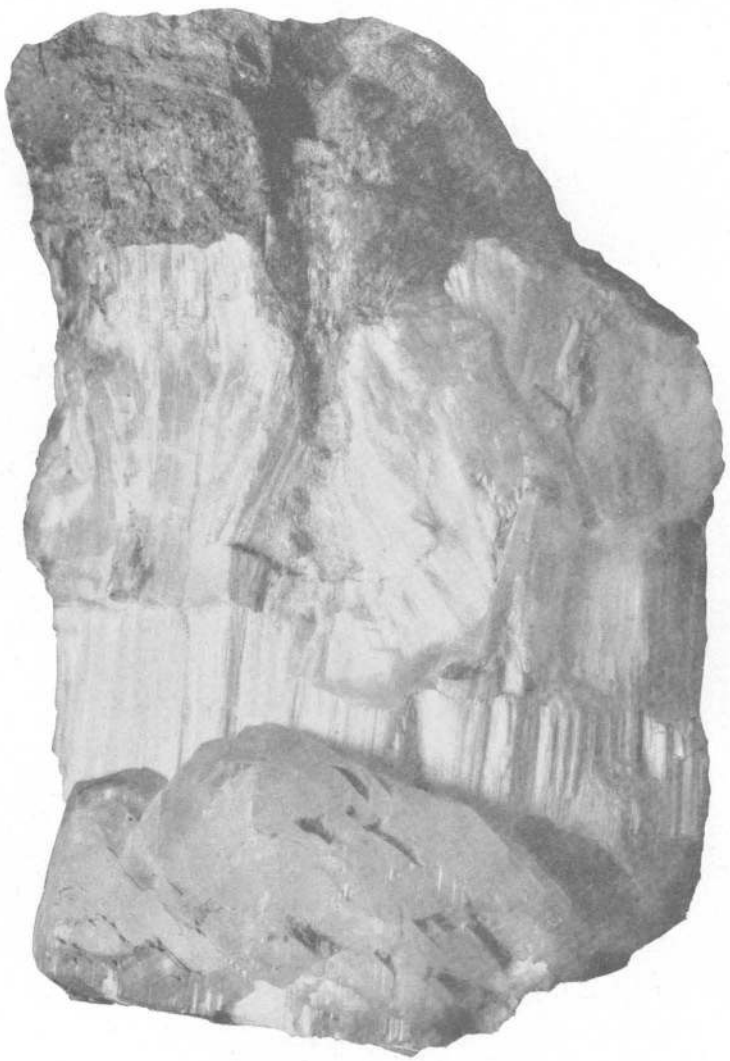

B. COLEMANITE AND ULEXITE IN CLAY ABOVE KERNITE DEPOSIT

U. S. National Museum catalog No. 95837. Natural size.

ULEXITE AND COLEMANITE

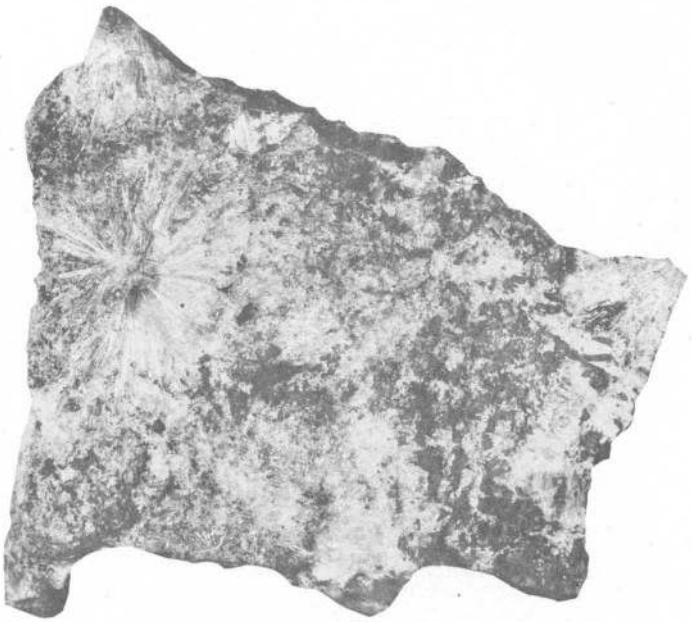

A. RADIATING GROUPS OF KRAMERITE CRYSTALS IN CLAY

U. S. National Museum catalog No. 95832. Natural size.

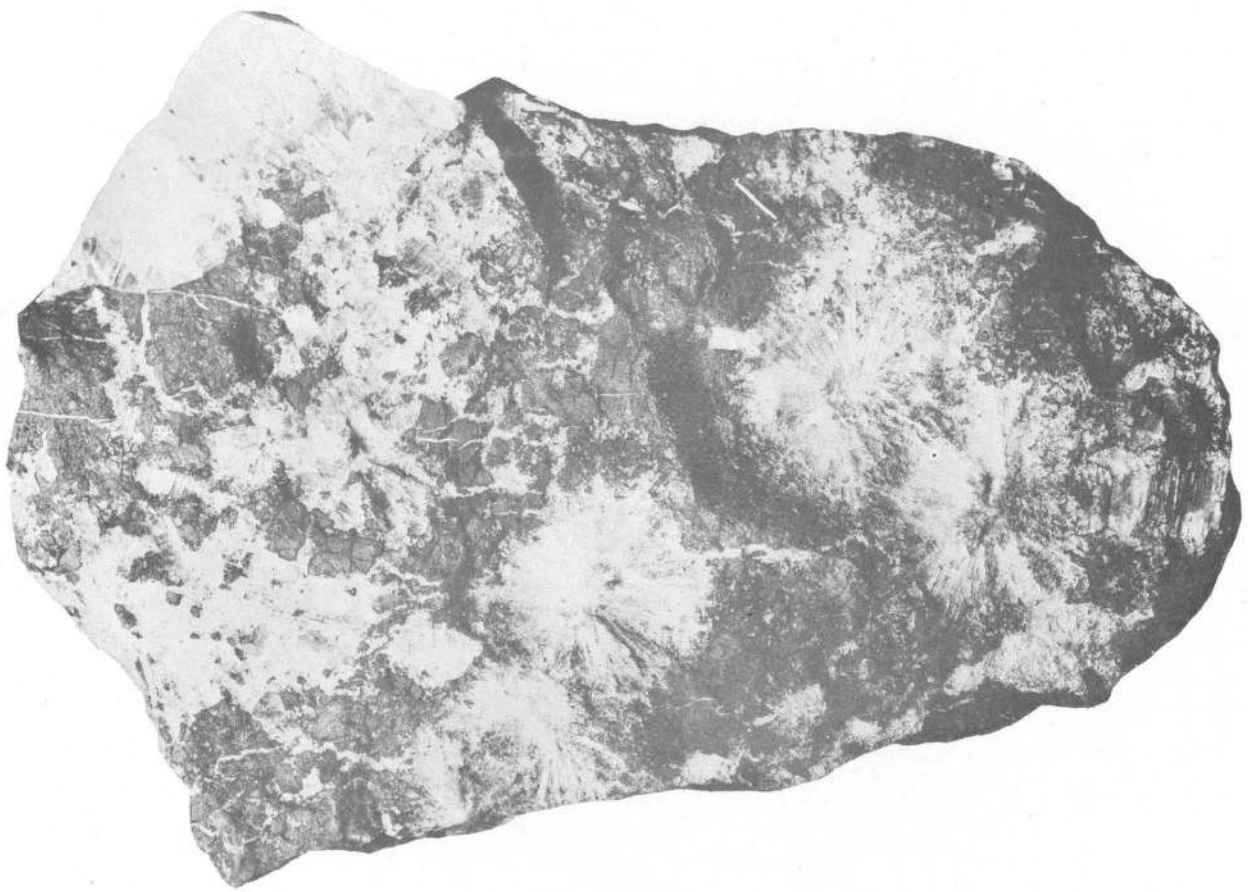

B. RADIATING GROUPS OF KRAMERITE CRYSTALS IN CLAY ASSOCIATED WITH KERNITE AND BORAX

U. S. National Museum catalog No. 95833. Natural size.

KRAMERITE

Many of the faces of the unit prism are rounded, and nearly all are striated vertically. Occasionally, in a distorted crystal (fig. 23), one pair of the faces are very much larger than the other pair and the crystal is flattened parallel to the prism.

The clinodome e (011) is the dominant terminal form on some crystals (fig. 24), or combined with t (101) it determines the terminal habit. It also functions as a relatively minor form, as shown in Figures 25 and 26. It is present on all crystals measured except one. Although not shown in the drawing of crystal 14 (fig. 23), it is present as a minute face, giving no reflection. The measurements of e (011) were used for the calculation of the axial elements of kramerite.

zone [$\bar{1}$01]. Usually the faces of d ($\bar{1}$01) are very small, as on crystal 6, shown in Figure 24.

The positive pyramid p (111) forms the dominant terminal form on some crystals (figs. 21 and 23) and even where accompanied by large faces of other forms still asserts its dominant character (figs. 25 and 26). The two faces of the form are commonly not of equal size. (See figs. 23, 25, and 26.) Only rarely is any face of the unit pyramid minute.

The negative pyramid o ($\bar{1}$11), the least common of all the forms, is always very small in its development. The reflections were hardly discernible but serve to determine the form. Its largest observed occurrence is shown on crystal 11, Figure 26.

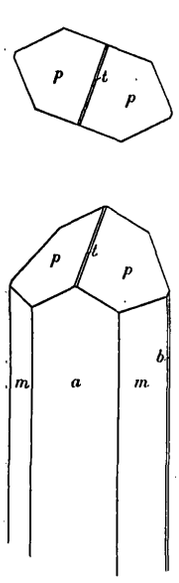

FIGURE 21.—Kramerite crystal 12. Dominant terminal form is p (111) with t (101) as long, narrow face. No other form present on crystal. All the measured crystals of kramerite are less than 1 millimeter thick

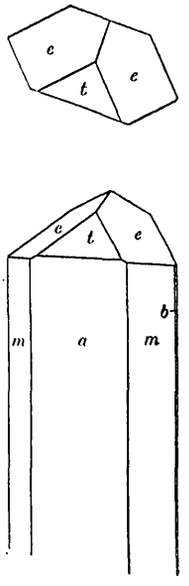

FIGURE 22.—Kramerite crystals 4 and 8. The clinodome e (011) is the dominant terminal form, with a large triangular development of t (101). Another crystal (No. 6, fig. 24), with e (011) the dominant terminal face, does not show t (101). Neither crystal 4 nor 8 shows any other form

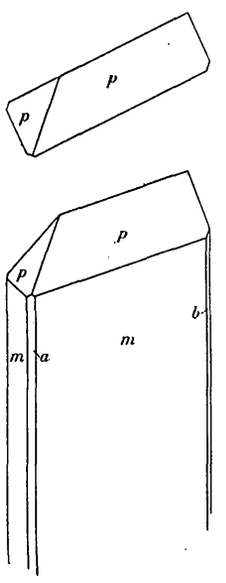

FIGURE 23.—Kramerite crystal 14. Distorted by unequal development of the prism faces, the crystal being flattened parallel to one pair. The clinopinacoid is larger than usual. The pyramid is the dominant terminal form, the crystal also having, though not shown in the drawing, single very minute faces of e (011) and o ($\bar{1}$11)

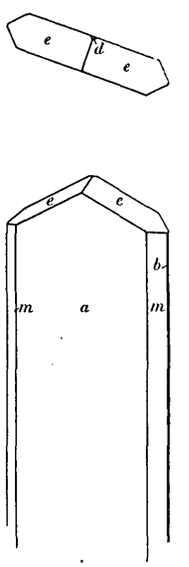

FIGURE 24.—Kramerite crystal 6. Flattened parallel to the orthopinacoid a, with e (011) the dominant terminal form and with a minute face of d ($\bar{1}$01)

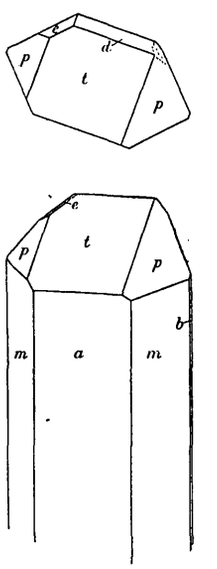

FIGURE 25.—Kramerite crystal 13. Slightly distorted crystal, showing large square face of t (101), with medium-sized faces of p (111) and smaller faces of e (011) and d ($\bar{1}$01). The only crystal on which the negative orthodome d reached any size. Shows all the kramerite forms except o ($\bar{1}$11)

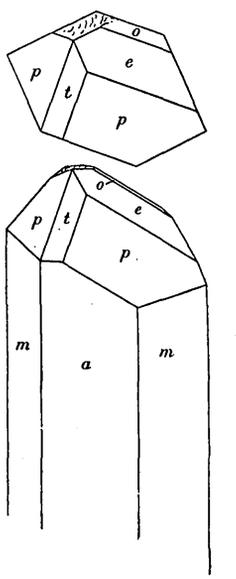

FIGURE 26.—Kramerite crystal 11. Another distorted crystal with t (101), e (011), p (111), and o ($\bar{1}$11). This face of o is larger than usual. The only crystal found not showing the clinopinacoid b. A minute face of d ($\bar{1}$01), not shown in the drawing, is present on the crystal

The positive orthodome t (101) varies considerably in size and relative dominance. It may be almost the largest terminal form, as in Figure 25, when it has a square shape due to p (111) being the other chief terminal form, or it is triangular if e (011) is the other chief terminal form. On other crystals the face becomes narrower (fig. 26), grading into a mere line face between the faces of p (111), as shown in Figure 21. It is present on about three-quarters of the crystals measured.

The negative orthodome d ($\bar{1}$01) is only about half as frequent in its occurrence as the positive dome. On crystal 13 (fig. 25) it is relatively large, the positive dome, with p, giving a long intersectional edge in the

The combinations observed on the 14 crystals measured are as follows:

Combinations on crystals of kramerite

Form	Percentage of occurrence	1	2	3	4	5	6	7	8	9	10	11	12	13	14
a (100)	100	a	a	a	a	a	a	a	a	a	a	a	a	a	a
m (110)	100	m	m	m	m	m	m	m	m	m	m	m	m	m	m
b (010)	93	b	b	b	b	b	b	b	b	b	b	--	b	b	b
e (011)	93	e	e	e	e	e	e	e	e	e	e	e	--	e	e
t (101)	71	t	t	--	t	t	--	t	t	t	--	t	t	t	-----
d ($\bar{1}$01)	43	--	--	d	--	d	d	d	--	--	--	d	--	d	-----
p (111)	71	p	p	p	--	p	--	--	--	p	p	p	p	p	p
o ($\bar{1}$11)	29	--	o	o	--	--	--	--	--	--	--	o	--	--	o

No measured crystal showed all the forms, but five crystals showed all the forms but one. Some of the faces were exceedingly minute, giving no reflection, and it is possible that some such forms missed recognition.

DESCRIPTION OF CRYSTALS

The crystals are all of long prismatic habit, the ratio of length to thickness being about 50 : 1. Many of the crystals are of nearly equal thickness in all horizontal directions; usually there is a slight flattening parallel to the orthopinacoid so that the crystal is a little longer in the direction of the *b* axis than in that of the *a* axis. A few are considerably flattened parallel to *a* (100) and rarely, by distortion, flattened parallel to one set of prism faces. (See fig. 23.) No twinning was observed on any of the crystals. The simple termination *e* and *t*, as shown in Figure 22, illustrates one type, as shown by crystals 4, 8, and 9. Another simple type is terminated dominantly by *p* (figs. 21 and 23), as shown by crystals 12 and 14. The drawings of Figures 25 and 26 are shown in the distorted condition in which the faces actually occur. Many of the crystals show a combination lying between the two drawings, with reference to the size and distribution of the terminal faces. Where only *e* is the chief terminal form, as in crystal 6 (fig. 24), the crystal is likely to be flattened parallel to the orthopinacoid.

CHEMICAL COMPOSITION

PYROGNOSTICS

When heated in a closed tube, kramerite decrepitates, giving off water, turns opaque white, swells slightly, and fuses imperfectly to a clinkerlike mass. The decrepitation is not as violent as with the compact fibrous ulexite, but the swelling is greater, ulexite showing hardly any swelling. When heated in the blowpipe flame, a crystal of kramerite readily fuses to a clear bubbly glass, giving a yellow flame. Kramerite is not soluble in water, either hot or cold, but is attacked by both.

ANALYSIS

The samples analyzed were prepared by crushing and hand picking. The results obtained with the first sample analyzed, in triplicate, are shown in the following table under "Hand picked, not washed." The prisms of kramerite penetrate all the associated minerals, and so small particles of borax may have remained in the sample, attached to or included between some of the prisms. Most of the glassy borax and all of the easily cleavable kernite was, however, readily removed. A small percentage of clay, both attached and included in the prisms, could not well be removed. The sample was dissolved in warm hydrochloric acid, which partly attacked the clay. For the B_2O_3 determinations (by titration), cold acid was used as a solvent.

A second sample was prepared after crushing and hand picking, by washing it for a few minutes with an excess of cold water, sufficient to dissolve any small quantity of borax that may have remained in the sample after careful picking.

The sample was small, and B_2O_3 was not determined in it. Both analyses yield closely the same formula, namely, $Na_2O.2CaO.5B_2O_3.10H_2O$.

Analyses of kramerite

[W. T. Schaller, analyst]

	Hand picked, not washed				Washed with cold water
	1	2	3	Average	
SiO_2, soluble in HCl	0. 61	0. 52	Not det.	0. 57	------
Al_2O_3, soluble in HCl	. 38	. 39	0. 49	. 42	------
Insoluble in HCl	1. 82	1. 85	1. 55	1. 74	0. 84
Na_2O	8. 19	8. 28	8. 56	8. 34	8. 05
CaO	15. 25	15. 07	15. 02	15. 11	15. 29
B_2O_3	49. 24	49. 52	49. 30	49. 35	[a] 50. 30
H_2O (total)	25. 44	25. 23	25. 52	25. 40	25. 52
	------	------	--------	100. 93	100. 00

[a] By difference.

A little potash was detected spectroscopically, but no chemical reaction was obtained for magnesia, sulphate, chloride, carbonate, or phosphate. The first sample, as analyzed, contained 2.73 per cent of anhydrous clay, which amounts to 3.10 per cent of clay, on the assumption of a water content of 12 per cent in the clay. Deducting this impurity and recalculating the analysis to a summation of 100 per cent gives the results obtained under 1 in the table below. Under 2 is given the analysis of the water-washed sample, with the insoluble clay deducted, recalculated to a summation of 100 per cent. In the third column is shown the calculated composition of the formula $Na_2O.2CaO.5B_2O_3.10H_2O$.

Analyses of kramerite, with insoluble matter deducted

	Not washed	Washed	Calculated
Na_2O	8. 53	8. 12	8. 83
CaO	15. 45	15. 42	15. 98
B_2O_3	50. 44	50. 73	49. 56
H_2O	25. 58	25. 73	25. 63
	100. 00	100. 00	100. 00

The ratios obtained from these analyses are as follows:

Ratios of analyses of kramerite

	Not washed		Washed	
Na_2O	0. 1376	0. 97 or 1×0. 97	0. 1310	0. 92 or 1×0. 92
CaO	0. 2754	1. 94 or 2×0. 97	0. 2748	1. 93 or 2×0. 96
B_2O_3	0. 7247	5. 10 or 5×1. 02	0. 7289	5. 12 or 5×1. 02
H_2O	1. 4211	10. 00 or 10×1. 00	1. 4294	10. 03 or 10×1. 00

These ratios clearly show the correctness of the formula $Na_2O.2CaO.5B_2O_3.10H_2O$.

The loss of water at different temperatures is as follows:

Loss of water of kramerite at increasing temperature

Temperature (°C.)	Loss (per cent)		Per cent of total water lost at each increase
	At each increase	Total	
107	5. 44	5. 44	22
122	2. 75	8. 19	11
150	2. 25	10. 44	9
179	4. 00	14. 44	16
200	----------	14. 44	----------
280	5. 30	19. 74	21
334	2. 83	22. 57	11
Ignition	2. 66	25. 23	10
	25. 23	----------	100

With a little over a fifth (possibly a fourth) of the water going off at 107°, the remainder of the water goes in many individual steps, approximating closely to a molecule at a time for many of the steps.

Although the mineral is not sufficiently soluble in water to give a clear solution, it is attacked by both cold and hot water, the amount of the differential solution being as follows:

Differential solution of Na_2O and CaO in kramerite, with water

[1 gram of mineral treated with 200 cubic centimeters of water over night]

	Na_2O		CaO	
	Per cent	Per cent of total	Per cent	Per cent of total
Soluble in cold water	1. 13	13	0. 47	3
Soluble in hot water	5. 30	62	9. 28	62
Soluble in hot HCl	2. 13	25	5. 27	35
	8. 56	100	15. 02	100

With cold water, more soda than calcium goes into solution, or else it goes faster; in hot water the same relative quantity of each dissolves. On the average about 70 per cent of the bases will be dissolved by hot water. About 1 gram of the powdered mineral was kept in a flask with 200 cubic centimeters of hot water on the steam bath (about 90°) for a week, but complete solution was not effected.

The establishment of the composition of kramerite determines definitely the existence of two hydrates of this type of compound—namely,

$Na_2O.2CaO.5B_2O_3.10H_2O$, or $H_{10}NaCaB_5O_{14}$, kramerite.
$Na_2O.2CaO.5B_2O_3.16H_2O$, or $H_{16}NaCaB_5O_{17}$, ulexite.

Apparently the lower hydrate prepared by Van't Hoff [6] is a third member of this group. But as stated in the next paragraphs, the supposedly 8-hydrate found by him—namely, $Na_2O.2CaO.5B_2O_3.8H_2O$—is probably the 10-hydrate and identical with kramerite.

Ulexite is stable up to about 60°, according to Van't Hoff, breaking down above this temperature into sodium borate and calcium borates (pandermite or colemanite, depending on the other salts present and character of inoculation).

SYNTHESIS

The lower hydrate prepared by Van't Hoff was formed by heating a mixture of two parts of ulexite and one of borax to a temperature slightly over 60°. The experiment was undertaken in an attempt to make franklandite, which was supposed to have the composition expressed by the formula $2Na_2O.2CaO.6B_2O_3.15H_2O$ (but which was shown by Van't Hoff to be identical with ulexite). He obtained a new compound, in needlelike crystals, to which, on the basis of analysis, he ascribed the formula $Na_2O.2CaO.5B_2O_3.8H_2O$.

In repeating the experiment as described by Van't Hoff except that the sealed tube was heated in the steam bath (about 90°) instead of being heated only slightly over 60°, a saturated solution of sodium chloride was introduced into the mixture of two parts of ulexite and one of borax. After a week's heating the insoluble mass in the tube (the soluble part being brilliant octahedral crystals of $Na_2O.2B_2O_3.5H_2O$—artificial tincalconite) was well washed with water and then air dried. It consisted of a finely fibrous uniform mass, whose optical properties showed that it was artificial kramerite, as follows:

	Artificial product	Kramerite
α	1. 517	1. 515
γ	1. 542	1. 544
Elongation	+	+
Extinction	15°	15°

An analysis of the air-dried artificial preparation yielded a total water content of 26.04 per cent, of which 4.45 per cent was given off on heating to 107° for three hours, leaving 21.59 per cent given off at higher temperature, a content practically identical with that found by Van't Hoff after washing and drying (21.2 per cent). As Van't Hoff gives no details as to how he dried the sample nor at what temperature, it is believed that his

[6] Van't Hoff, J. H., Franklandite und eine neue, dem Boronatrocalcite verwandte Verbindung: Preuss. Akad. Wiss. Sitzungsber., 1907, p. 303.

preparation was artificial kramerite but that on drying before analysis, some of the water was driven off.

The analysis of the artificial kramerite yielded the following figures.

Analysis of artificial kramerite

[W. T. Schaller, analyst]

	Artificial	Calculated
Na_2O	9. 17	8. 83
CaO	15. 87	15. 98
B_2O_3	[a] 48. 92	49. 56
H_2O	26. 04	25. 63
	100. 00	100. 00

[a] By difference.

KERNITE

OCCURRENCE

Kernite has been found only on the east side of the Kramer borate field in Kern County, close to the San Bernardino County line. The mineral was first obtained from the Discovery shaft of the Pacific Coast Borax Co.'s mine, known as the Baker deposit, in sec. 24, T. 11 N., R. 8 W. A later shaft, the Osborne shaft, also in kernite, is 382 feet east of the Discovery shaft, in sec. 19, T. 11 N., R. 7 W. Apparently no kernite was found below the earlier-discovered deposits of colemanite and ulexite lying a few miles to the west, chiefly in secs. 14 and 22, T. 11 N., R. 8 W.

When visited in September, 1927, the workings were reported by Mr. Rasor to show a thickness of the kernite deposit of a little over 100 feet and a lateral extent in two directions of at least 600 to 700 feet each way, the deposit not being penetrated in several places. The horizontal dimensions given are therefore a minimum.

The deposit consists of clay in which are embedded seams and crystals of kernite. (See pl. 27.) The clay, described on page 165, is bedded and faulted and is probably composite in character. The extreme abundance of kernite, its large crystals, its perfect cleavage, and its clearness and transparency render the occurrence one of almost unique character as well as of striking beauty. For many feet kernite is the only borate mineral seen. In places it is so abundant that the clay matrix becomes almost negligible in amount. Although the writer has no figures available to determine the quantity of kernite present he would estimate that not less than 75 per cent of the deposit is formed of this striking mineral. Large bodies of massive borax were encountered, but the proportion of borax to kernite is very small. With a thickness of 100 feet and a lateral extent in two directions of 600 feet each, a rectangular body having a kernite content of 75 per cent would contain at least 1,600,000 short tons of kernite. This figure would be equivalent to about 2,000,000 short tons of borax, as 1 ton of kernite, when dissolved in water, will upon crystallization yield 1.39 tons of borax. That the deposit is probably much larger is suggested by the published statement [7] that

> It appears that an important extension of the richest part of these deposits lies south of the property now being operated, and this new deposit is evidently under independent control. The discovery was made by borings and is situated about three-quarters of a mile southwest of the original shaft, in the northeast corner of sec. 24. According to authentic information, these borax deposits reveal a thick section of particularly pure kernite in the new area referred to, and a mining shaft is being rapidly sunk to develop this new deposit.

This same article states that the average daily shipment of crude kernite ore of high purity is 200 tons. It is shipped to Wilmington, near Los Angeles, where it is dissolved, the clay is filtered off, and the residue is recrystallized into borax.

According to report, the top of the kernite deposit is about 300 feet below the surface. Above the kernite the clay, as seen in dump specimens, is rich in seams of fibrous ulexite of a fine satin-spar appearance. Such an occurrence is shown in Plate 22, *A*. The ulexite seams, though apparently abundant, are only a few inches thick at most, to judge from the specimens collected from the dump. Colemanite also occurs with the ulexite above the kernite but apparently is not very abundant. A fine specimen presented to the United States National Museum by Mr. Rasor is shown in Plate 22, *B*. Mr. Rasor states that both colemanite and ulexite were found for a few feet below the kernite, but neither colemanite nor ulexite was seen anywhere in the kernite deposit by the writer. A bed of igneous rock is reported to lie beneath the borates, as in the occurrences a mile or two to the west.

The minerals associated with the kernite are few, comprising the minerals in the clay, borax, tincalconite, kramerite, calcite, realgar, and stibnite. In most of the deposit no other borate in quantity is associated with the kernite, but it is probable that very small quantities of borax, tincalconite, and kramerite are to be found throughout the deposit. A thin film of white opaque tincalconite coats some of the kernite crystals and also forms on many of the cleavage surfaces. Though not present in large amounts, it is very widespread in its occurrence.

Genetically the most interesting association of kernite and other borates occurs where the irregularly bounded crystals of kernite are embedded in massive borax. A sufficient number of such occurrences were noted to show that the relation is not unique. Such kernite crystals embedded in borax as were collected are irregular in shape (see fig. 33) and show no definite crystal faces, all the faces of *c* (001) and *a* (100) observed being cleavage faces. It is very probable, however, that crystals bounded by true faces (not

[7] Eng. and Min. Jour., vol. 125, p. 551, 1928.

cleavage) are present in the borax. The sides corresponding to the faces of the clinodome *e* (011) have a rough, dull appearance just like many of the kernite crystals embedded in the clay matrix. These kernite crystals in the borax reach a thickness of several inches. In the presence of borax kernite specimens (in the Washington laboratory) readily alter on the surface to tincalconite. This alteration is described below in connection with the chemical composition. In general appearance the kernite crystals in the borax matrix are identical with those in the clay matrix. When collected, the borax of these specimens was bright and glassy, but within a few months, in the Washington laboratory, the borax alters to tincalconite and part of the kernite undergoes a similar alteration, though very much more slowly.

In the mine kernite is most abundant as large crystals (pls. 24, *A*, and 27), though veins of cleavable kernite (pl. 24, *B*), as well as irregular masses, are likewise very abundant. The largest crystal noted, near the Discovery shaft, measured 8 feet (*c* axis) by 3 feet. Single crystals 2 to 3 feet thick are very common. As seen in the face of the tunnels, the exposed surface of the crystals is bounded by alternating faces of the cleavages *c* (001) and *a* (100). (See fig. 32.) By careful removal of the clay matrix it might be possible to obtain large crystals of kernite bounded by natural faces. One of the specimens of clay matrix contains abundant crystals averaging about 1 centimeter in thickness. By careful picking and removal of the clay, natural faces of forms in the orthodome zone—either *c* (001), *a* (100), or *D* ($\bar{1}01$)—can be seen to be present. The faces of the other terminal form—namely, the clinodome *e* (011)—are always dull and rounded. In fact, if only the kernite crystals embedded in the clay were available for the determination of the crystallographic elements, they could not be accurately determined. Fortunately, some excellent small crystals were found completely embedded in the large crystals of kernite, and these small crystals were removed by very careful cleaving of the large crystals and found to be bounded by smooth and brilliant faces whose measurements furnished the required angles for the calculation of the crystallographic constants. Small embedded crystals of kernite are also developed in some of the fracture zones of the larger cleavage pieces. The veins of kernite, several inches thick and 10 feet or more long, show an apparent fibrous structure either normal or slightly inclined to the walls. No definite genetic relation was established between these veins and the individual crystals, but many of the large irregular-shaped well-crystallized masses, showing consistent cleavage throughout, have what appear like vein feeders. Many of the crystals show no connecting or feeding veins and appear to be isolated in the clay, but the kernite is so abundant that it is difficult to show conclusively that these crystals are not connected to other masses or crystals by smaller veins. (See pl. 27.)

Much of the clay is richly seamed with veins of kernite, in both parallel and divergent groups. Many of the kernite veins follow the bedding of the clay, but many also cut across the bedding at all angles and swell and pinch and are most irregular in shape and size. "Eyes," disconnected or connected by the merest threadlike veins, such as are typical of quartz veins in schist or gneiss, were not seen. The kernite veins are commonly either nearly horizontal or have a small inclination. Vertical veins are not common.

Many veins of kernite have begun to form in the clay, with but a small percentage of the borate mineral present. At other places the kernite is more abundant, and many of the veins consist of nearly pure kernite, with a very small quantity of included clay. A set of such parallel veins in the clay is shown in Plate 24, *B;* the upper vein contains a minimum of clay, but clay greatly predominates in the lower veins. All the kernite veins in the specimen are nearly parallel, and the kernite itself is all in parallel position. It is believed that if the process of kernite formation had continued, practically all the clay would have been removed and a single vein of pure kernite would have resulted.

The fibrous structure shown by the veins is due to the excellent cleavages possessed by the mineral, which when well developed greatly simulate a fibrous structure. The cleavage of kernite is parallel to faces all lying in the orthodome zone. It is perfect parallel to two forms, the base *c* (001) and the orthopinacoid *a* (100), and imperfect parallel to the rear or negative unit orthodome *D* ($\bar{1}01$). These cleavages have a strong tendency to break down a crystal into a mass of fine fibers resembling a mass of tremolite asbestos. In places on the floor of the tunnels there will be a mass of such fibers of considerable thickness, and unless one breaks up a mass of solid kernite himself he finds it hard to believe that such a mass of fine fibers could develop from a solid piece of the mineral. The two cleavages are so perfect that very thin hairlike fibers several inches long can readily be cleaved off.

The general appearance of the large crystals, as seen in the mine (pl. 27, *B*), is illustrated by Plate 24, *A*, which shows a crystal nearly 9 centimeters high and 6 centimeters wide. The front is formed by alternating cleavages of *c* (001) and *a* (100), and the two rough faces of the clinodome *e* (011) show in part. Large crystals of similar shape are very abundant in the mine. Many of these have a distinct 6-sided appearance, suggesting that the clinopinacoid *b* (010) is present as a large face, although on the very small measured crystals, embedded in a large crystal, the clinopinacoid is a rare form and present only as a line face. On the large crystals seen in the mine the top angle between the two sloping faces is distinctly greater than 90°

and was estimated to be about 110°, which agrees with the calculated angle of 116° 14′ for *e* (011) ∧ *e*′ (0$\bar{1}$1).

Another mass of kernite is shown in Plate 25, *A*. This mass represents the irregular shape of much of the kernite in the mine, for where it is in contact with the clay matrix there is usually no definite crystal face present. This specimen shows a number of other relationships, for the mass of kernite contains a number of small veins of borax cutting right through the kernite. The relations, as shown in Plate 25, *A*, are illustrated and described in Figure 27. The seam of banded clay probably represents a harder and more resistant layer, which was difficult to replace by the borate minerals. A similar but smaller layer of such harder clay is seen on the extreme right of the specimen. These harder layers contain a little borax, whereas on each side of the larger layer, in the mixture of borax and clay, the borax is present in the largest quantity. It is in the kernite specimen here shown that the first small embedded crystals were found,

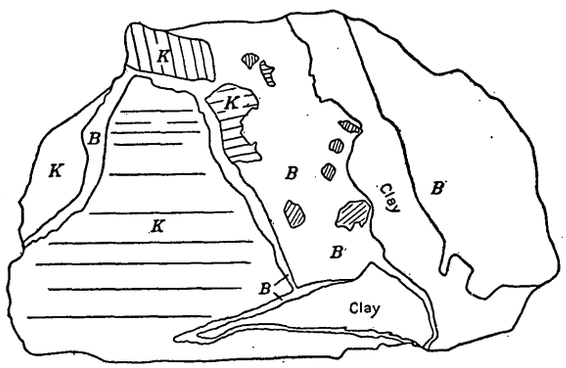

FIGURE 27.—Relations of kernite and borax. Explanatory of Plate 25, *A*. The seams of borax cutting kernite (K) are marked B. They are now coated by its dehydration product, tincalconite. The seam of clay, containing a little borax, which is harder and more compact than the other clay, is well shown in Plate 25, *A*

but since then such crystals have been observed in several other masses of the kernite.

PHYSICAL AND OPTICAL PROPERTIES

Kernite possesses a number of separation directions of varied perfection. Two cleavages are perfect, parallel to the base *c* (001) and the orthopinacoid *a* (100). A third direction of fair cleavage is parallel to *D* (1$\bar{0}$1). On some large cleavage fragments there is a suggestion of a poor cleavage after *e* (011), and a few fragments were found on which a cleaved surface parallel to this clinodome was observed. Several pieces also show a distinct fracture—it can hardly be called cleavage—after the clinopinacoid *b* (010), which yields irregular and not plane surfaces, some of which are fairly parallel to the *b* face.

The cleavage after the base *c* (001) is perhaps the best developed and easiest obtained. Many of its surfaces yield mirror-like reflections on the goniometer. Many of these cleavage surfaces also show a multitude of lines parallel to the intersection edge *c* (001) ∧ *e* (011). These may cover the entire surface of the *c* cleavage and suggest traces of planes of separation or of gliding or warping (or possibly twinning) parallel to *b* (010). They resemble the traces of parting planes seen on crystals of stibnite. Warping in this zone, *c e b*, is common for the kernite cleavage fragments, the pieces being warped or bent for several degrees; one long cleavage piece (19 centimeters long and 1 centimeter thick) was warped through an angle of nearly 4°. Thin cleavage pieces (after *c* (001)) can be bent through a small angle without breaking, quickly springing back on release of pressure. The difference between the *c* and *a* cleavages can be readily seen in pieces fractured parallel to *b* (010). On these pieces the cleavage after the base *c* is developed as innumerable closely spaced lines, giving almost a striated appearance to the surface, whereas the cleavage after *a* may show only as a few—perhaps three or four—well-developed lines.

The cleavage after *a* (100) is likewise perfect, and many surfaces yield similar mirror-like reflections. There is, however, more of a tendency to develop small fibers on this cleavage than on that after the base. The cleavage surfaces of *a* do not show the parting lines so characteristic of the basal cleavage.

The cleavage after *D* (1$\bar{0}$1) is decidedly fibrous. Whereas plates or sheets can be readily split off parallel to *D* (1$\bar{0}$1), their surfaces are not smooth and mirror-like but strongly fibrous, owing in part perhaps to the simultaneous development of the *a* and *c* cleavages. Most of the occurrences of the form *D* (1$\bar{0}$1) recorded on crystals 1 to 12 are cleavage faces.

The separation after *e* (011) can be classed only as very rare and not well developed, but the resultant faces are fairly plane and resemble a cleavage rather than a fracture. The separation after *b* (010) is better developed than that after *e* (011) and often shows on the *a* and *c* cleavages as strong cracks, but the resultant faces are never plane but always uneven, so that this separation should be classed as a fracture rather than a cleavage.

The multitude of lines on the basal cleavage, parallel to the intersection edge *c* (001) ∧ *e* (011), may result from warping, or gliding planes, or twinning (after *e* (011)). They can be produced by pressing a piece of kernite in the direction of the *b* axis. In fact, by clamping a cleavage fragment between two pieces of soft wood in a vise and gradually increasing the pressure, not only can these lines be readily developed, but the kernite fragment is so rigid that the two ends are forced into the wood for a considerable distance. By pressing or rolling a cleavage piece between the fingers in a direction at right angles to the *b* axis the mineral is easily broken into innumerable fibers, all three cleavages in the orthodome zone developing.

The hardness of kernite is 2½ but varies slightly on the different faces and in different directions. Calcite readily scratches kernite, and kernite readily

cuts gypsum. The average density obtained by suspending 12 clear fragments in diluted bromoform was 1.911, and a second group of 12 clear fragments gave an average of 1.904. Slight variation in the fragments is caused by the presence of minute traces of clay, of a minute quantity of adhering tincalconite, of the abundant inclusions of negative crystals (probably filled with some liquid), and of incipient cleavage cracks holding some air. The average of the two results, or 1.908, is probably close to the true density. This figure is slightly lower than the value first given, but being made on more abundant material, almost free from clay, is considered more accurate. Kernite is colorless, transparent. The white opaque appearance shown by some pieces is due to the presence of a film of tincalconite. The luster is vitreous but on a fibrous cleavage surface slightly satiny. The streak is white.

The optical axial plane is normal to the clinopinacoid b (010), X and Y lying in the plane of symmetry. The mineral is definitely negative, determined by the bar on a section normal to an optic axis. Sections parallel to a (100) show an inclined interference figure, of negative character. Therefore, b axis = Z, $Bx_o \perp$ (010). On a section parallel to the clinopinacoid b (010), $X \wedge 001$ cleavage = 37½°; $X \wedge c$ axis (a cleavage) = 70½°. Therefore a positive orthodome, with a ρ angle of 70½, would be normal to the acute bisectrix. On the a cleavage the axial plane is tilted 20°; on the c cleavage the tilt is 52½°. The a cleavage will therefore show the interference figure inclined to one side, whereas the c cleavage does not yield a figure. The optical orientation of kernite is shown in Figure 28.

Measurement of the refractive indices by the oil-immersion method gave the following results:

Refractive indices of kernerite

	Schaller	Ross	Henderson	Average	Artificial kernite
α	1. 454	1. 454	1. 455	1. 454	1. 455
β	1. 471	1. 472	1. 473	1. 472	1. 472
γ	1. 487	1. 489	1. 488	1. 488	1. 487
B	. 033	. 035	. 033	. 034	. 032

The axial angle, 2V, was measured as 80°. The angle in air, 2E, is 142°. Dispersion distinct, $\rho > v$.

CRYSTALLOGRAPHY

GENERAL DESCRIPTION

From the small cleavage fragment first received from Mr. Gale it was concluded [8] that kernite was orthorhombic and that the cleavage was prismatic. When more material was received it was noticed that the two pairs of cleavage faces showed considerable differences, and it was soon seen that kernite is monoclinic and that the cleavages belong to forms in the orthodome zone. This conclusion was independently arrived at by Dr. C. Hlawatsch,[9] of Vienna, who also called attention to the marked difference of the etch figures on the two cleavages. The specimens of kernite that had been distributed were cleavage pieces and showed an elongation parallel to the cleavages. This direction, originally chosen as the c axis when the mineral was thought to be orthorhombic with prismatic cleavage, is the direction of the b axis of the monoclinic crystals, and although the cleavage pieces are elongated in this direction, the crystals themselves are not, being more nearly equant (pl. 24, A), with generally a slight elongation in the vertical direction. An examination of the outlines presented by many small crystals embedded in the clay matrix, as given in Figure 33, shows that elongation of the crystals parallel to the b axis is very rare, the common elongation being in the direction of the c axis, as also illustrated in Figure 32, which shows, too, how a cleavage fragment would lie horizontally in the crystal and have an elongation normal to the elongation of the crystal itself.

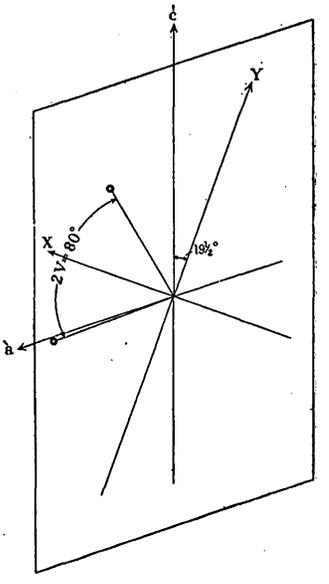

FIGURE 28.—Optical orientation of kernite

The large crystals seen in the mine have the appearance of the one shown in Plate 24, A, with various modifications. An attempt to show the actual appearance of a kernite crystal unusually elongated parallel to the c axis and embedded in the clay matrix is given in Figure 32, where no actual crystal faces are present but the exposed front side of the crystal is bounded by alternating cleavage faces of the basal pinacoid c (001) and the orthopinacoid a (100). Both of these cleavages are so nearly perfect that it is difficult to handle a piece or crystal of kernite without developing one or both of them.

Several of the cleavage fragments received later from Mr. Gale showed a number of narrow line-face forms, all in the orthodome zone, but no other terminal faces could be found. The material collected by the writer contained several pieces which showed small embedded crystals of kernite in the larger cleavage fragments. These small crystals were carefully removed, and a few terminated crystals were obtained. The measure-

[8] Schaller, W. T., Kernite, a new sodium borate: Am. Mineralogist, vol. 12, p. 24, 1927.

[9] Personal communication.

ments of these small terminated crystals afforded a basis for deciphering the crystallography of kernite. The perfect cleavages of the mineral made it extremely difficult to remove and to handle these small crystals. On the other hand, it is doubtful if they could have been obtained from the inside of the larger masses but for this perfect cleavage. The crystal measurements were made, therefore, on a composite lot of cleavage pieces showing only very narrow line faces as natural crystal faces, on cleaved fragments of terminated crystals, and on a very few complete crystals.

It was soon seen that the crystals of kernite were bounded by faces in only two zones—one, the dominant zone, rich in faces and heavily striated, and the other zone, at right angles to it, showing essentially only one large form, with four faces all around the crystal, not striated. The cleavages were readily seen to lie in the striated zone. Goniometric measurements showed that many forms were present in the striated zone, that the single form seen in the second zone was the dominant one and the few other forms found in this zone were represented only by very narrow faces. No other forms not shown in one of these two zones were observed on any of the crystals.

A total of 20 crystals or cleavage fragments were measured. Of these, Nos. 1 to 12 were cleavage pieces that showed forms additional to the cleavage faces of *c* (001) and *a* (100). Fragment No. 9 was part of No. 8, and fragment No. 12 was part of No. 11. Nos. 13 and 14 were cleavage fragments of a crystal, and Nos. 16, 17, and 18 were cleavage pieces of one crystal which broke or cleaved into several pieces on removal from its kernite matrix.

Measurements were therefore made on three complete crystals (Nos. 15, 19, 20), two other crystals separated into two (Nos. 13 and 14) and three pieces (Nos. 16, 17, 18), respectively, and 10 cleavage fragments. Where it is necessary to refer to fragments 13 and 14 collectively, they will be called crystal 13, and fragments 16, 17, and 18 will be called crystal 16.

The crystallography of kernite, with regard to the development and relationship of crystal forms and faces, and the accompanying crystal drawings are therefore based on only five complete crystals. Several more such embedded crystals were seen, but they showed no essential differences from those measured.

Some of the crystal drawings represent an idealized type of combination, rather than a single crystal measured, owing in part to the fact that most of the crystals were somewhat distorted and showed differences in combinations of forms and development of faces in front and rear, and owing also to the strong striations, embayments, and irregular development that most of them showed.

The crystals of kernite can be referred to two fundamental types, both of the same general habit, which are illustrated in Figures 29 and 30. The only difference between the two drawings is that in Figure 29 the dominant form is the orthopinacoid *a* (100), whereas in Figure 30 the dominant form is the rear negative dome *D* ($\bar{1}01$). The only other forms shown are the base *c* (001) and the clinodome *e* (011). A combination of these two developments, showing both *a* (100) and *D* ($\bar{1}01$) is shown in Figure 31, wherein is also illustrated another characteristic—namely, that one basal pinacoid shows its greatest development in a direction normal to that of the other basal pinacoid. Either one of these three combinations, modified by other forms, represents the habit of all the crystals measured, although none of the measured crystals were as simple in their combinations as those shown in Figures 29, 30, and 31. Figures 35, 36, and 40 represent variations and modifications of Figure 29; Figure 37 represents variations and modifications of Figure 30; and Figures 38 and 39 show various modifications of the habit and combination shown in Figure 31.

It is very probable, however, that many of the large crystals of kernite in the mine will show a simple combination, such as is depicted in Figures 29 to 31. The

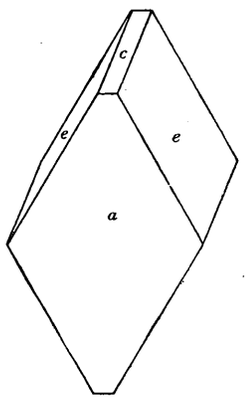

FIGURE 29.—Fundamental simple type of kernite crystal, with large development of *a* (100). Other forms are *c* (001) and *e* (011)

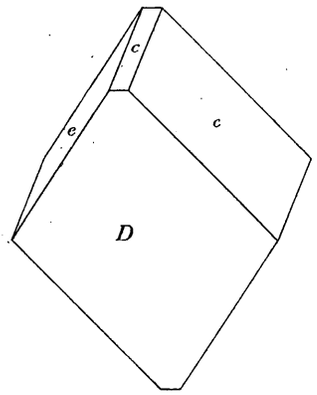

FIGURE 30.—Fundamental simple type of kernite crystal, with large development of *D* ($\bar{1}01$)

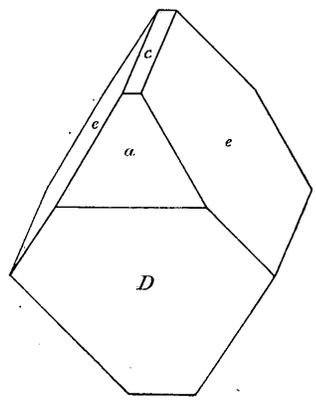

FIGURE 31.—Combination of the two types shown in Figures 29 and 30. Forms *a* (100), *c* (001), *e* (011), *D* ($\bar{1}01$)

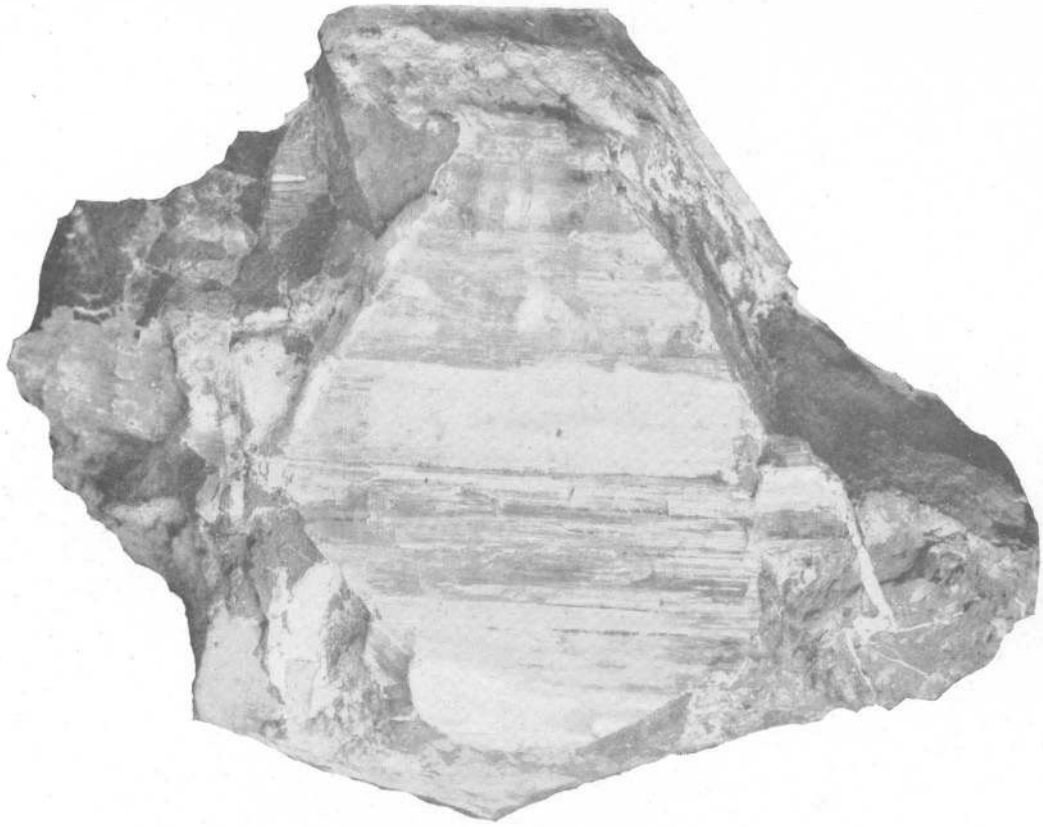

A. KERNITE CRYSTAL IN CLAY

U. S. National Museum catalog No. 95834. Natural size.

B. SEAMS OF KERNITE IN CLAY

U. S. National Museum catalog No. 95835. Natural size.

KERNITE

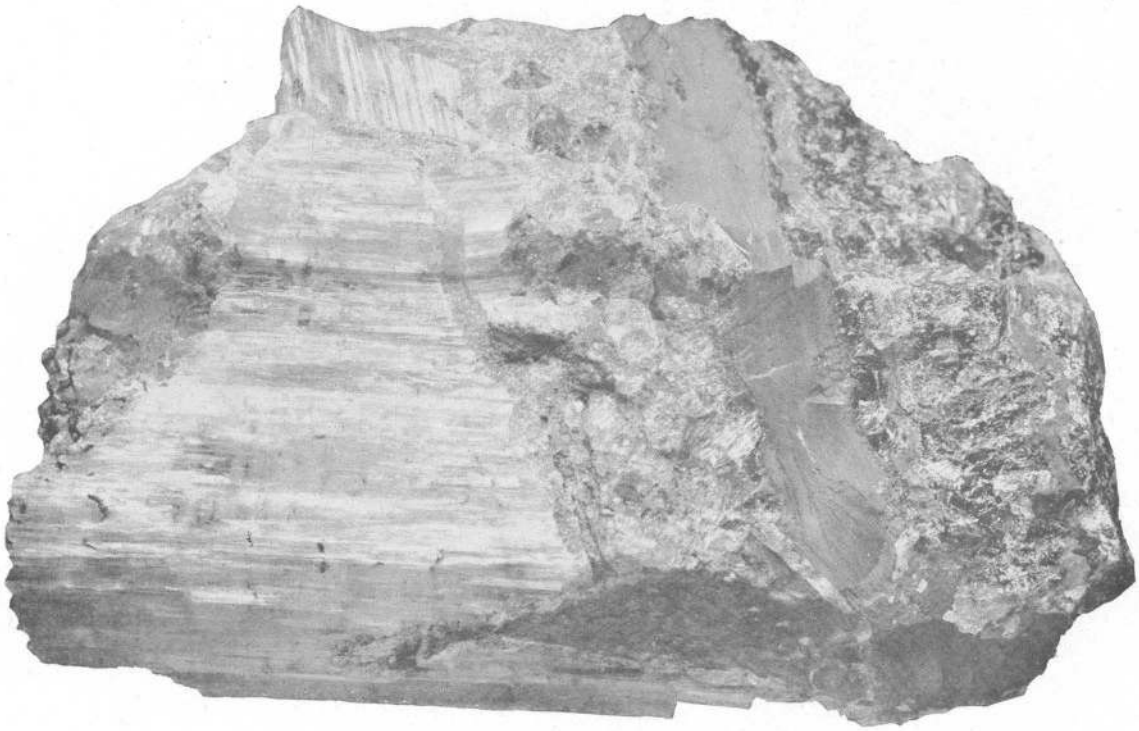

A. KERNITE WITH SEAMS OF BORAX AND TINCALCONITE

Relationships explained by Figure 27. U. S. National Museum catalog No. 95835. Natural size.

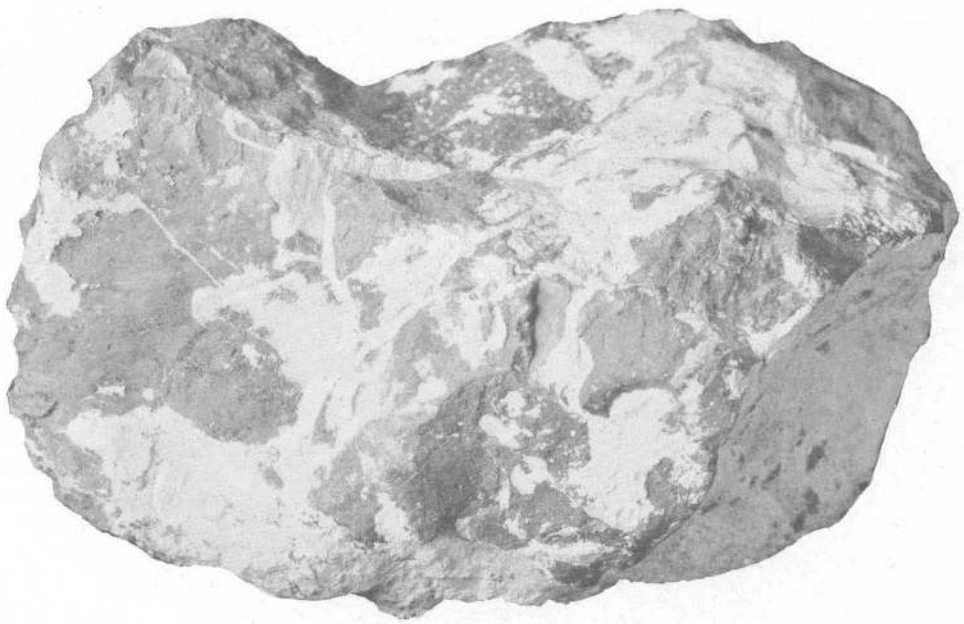

B. TINCALCONITE

Back side of specimen illustrated in Plate 24, *A*. U. S. National Museum catalog No. 95834. Natural size.

KERNITE WITH BORAX AND TINCALCONITE

actual form habit of the large crystals embedded in the clay is very difficult to determine, as in breaking them out the perfect cleavages parallel to *c* (001) and to *a* (100) readily develop and the real crystal face forming the external boundary of the crystal is lost. The crystal shown in Plate 24, *A*, probably had a form combination shown by either Figure 29, 30, or 31. Owing to this development of the two perfect cleavages the exposed surface of the crystal in the clay shows many steplike alternations of the two cleavages (*a* and *c*), together with a highly striated surface, such as is shown in Figure 32, which is an attempt to illustrate the appearance of such a crystal embedded in the clay matrix. All the faces lettered *c* and *a* are cleavage faces. The two clinodomes, *e* (011) and *e'* ($0\bar{1}1$), are probably represented, but both their surfaces are uneven and dull. The crystal shown in Figure 32 is also considerably elongated parallel to the *c* axis, an occurrence not at all rare.

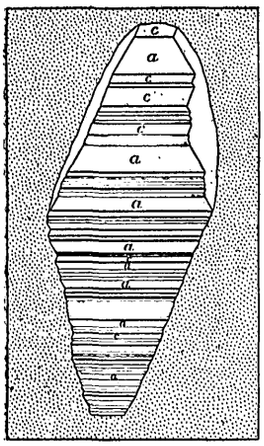

FIGURE 32.—Appearance of kernite crystal in clay matrix, showing the alternation and repeated cleavage faces of *c* (001) and of *a* (100)

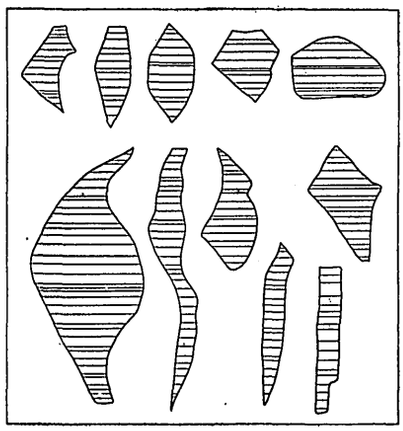

FIGURE 33.—Various shapes outlined by kernite crystals embedded in the clay matrix

Many of the crystals in the clay matrix are bounded by rounded surfaces, so that as viewed on the broken surface bounded by the cleavages, the crystals appear of various shapes and configurations. Figure 33 shows a collection of such shapes as were observed on a specimen of the clay matrix containing many of these small kernite crystals, averaging from about 1 to 3 centimeters high. Some of these outlines suggest the presence of a large face of the clinopinacoid *b* (010), especially the sketch in the lower right-hand corner of Figure 33, but none of the crystals measured showed any large development of this crystal form.

The crystals measured, Nos. 13, 15, 16, 19, and 20, averaged several millimeters in size. Thus crystal 15 is about 2 millimeters high, 1½ millimeters wide, and 1 millimeter thick; crystal 19 is about 2½ by 2 by 1 millimeter; crystal 20 is 3 millimeters high. The crystal whose cleaved fragments form Nos. 16, 17, and 18 was probably at least 5 millimeters high, and after the crystallographic measurements were made a crystal embedded in kernite was found that is about 1 centimeter high.

All the measured and observed crystals are simple and not twinned, but on a large specimen 2 feet thick partial development of crystal faces shows twins of kernite (after *e* (011)). (See fig. 41.)

Kernite being monoclinic, the orthodome zone remains fixed in any orientation that might be chosen. But the crystal can be revolved on the *b* axis into any position, and as only one other form, lettered *e* in the drawings, reaches any development, the allocation of this form determines the orientation. No conclusive reason could be found for decisively making either of the two perfect cleavages the basal pinacoid. The only important form present on these crystals outside of the orthodome zone lies in the zone *b* (010) $\wedge$ one of the perfect cleavages. This form then becomes either the unit prism or the unit clinodome. Both orientations were considered for a while, and it was finally decided to choose the clinodome, chiefly because the habit of the crystals could be best shown in drawings in this position, and the appearance in the mine—as shown in Plate 24, *A*, for example—could then be better compared with the drawings. The simplicity of the indices of the crystal forms in the two orientations remains the same. The change simply amounts to an interchange of the basal or orthopinacoids, with a revolution of the crystal through 180°, so as to keep the angle $001 \wedge 100$ less than 90°.

CALCULATION OF ELEMENTS

Although many crystal forms are present in kernite, a total of 36 having been determined, the crystallographic elements were calculated from the measurements of only three forms. The finding of more and perhaps better material and the measurement of its angles may give more accurate figures than those here presented. The measurements of the angle between the two perfect cleavages have given consistent results, and so have readings on the natural faces of *c* (001). The average of the 25 best readings of ρ, finally taken, is 18° 52′. This average is derived from 2 readings of 18° 49′, 3 of 18° 50′, 3 of 18° 51′, 10 of 18° 52′, 5 of 18° 53′, 1 of 18° 54′, and 1 of 18° 55′. This is the same value (or more accurately, its complement) originally obtained and given as the prismatic cleavage angle $m \wedge m = 71°\ 08'$, when kernite was considered orthorhombic. The cleavage angle ($001 \wedge 100$ = complement of ρ (001)) was also again measured directly on 10 separate cleavage fragments, the minutes thus found being 9, 7, 7, 7, 10, 6, 8½, 7, 8, 8, an average of 7¾—that is, 71° 07¾′, or a ρ value of 18° 52¼′. The angle β (or μ if β is taken as greater than 90°) for kernite is then 71° 08′, or ρ (001) = 18° 52′. The fair or good reflections from all the cleavage

and natural faces gave a ρ value for c (001) ranging from 18° 45′ to 18° 56′. The average of all such fair to good readings is 18° 51′+.

Many less good readings were obtained on e (011) than on c (001), because the faces were not as smooth and brilliant. The crystals were all measured in the orientation where e (011) was taken as the unit prism, so that the figures here given represent the ϕ value—that is, the angle between e and the clinopinacoid b (010), when e is taken as the unit prism (110). Some of the faces of e also gave two reflections, which reached a maximum difference of half a degree. However, by proper observation and adjustment, the following measurements of the angle $e/\wedge b$ (010), representing e taken as (110), were obtained:

°	′	°	′	°	′	°	′
31	35	31	43	31	53	32	07
31	35	31	44	31	54	32	08
31	36	31	45	32	01	32	10
31	38	31	46	32	02	32	10
31	38	31	48	32	04	32	12
31	40	31	51	32	05	32	12
31	41	31	53	32	06		

The properly weighted average of these 27 measurements is 31° 53′. As the angle 001/\010 is 90°, the complement of this average, or 58° 07′, is the angle c (001)/\e (011). This value, with the ρ value of 18° 52′ for c (001), gives a basis for calculating the c axis of kernite, which is found to be 1.6989.

The ρ angle for the rear negative unit dome D ($\bar{1}01$), in the position where e is taken as the unit prism, was found to average 31′ 12°, based on the following 13 measurements:

°	′	°	′	°	′	°	′
30	56	31	11	31	12	31	17
30	58	31	11	31	14	31	22
31	09	31	11	31	15	31	26
31	11						

The average of all measurements, ranging from 29° 54′ to 31° 40′, is 31° 10′, or nearly the same. The average of the best readings of large faces or cleavages, giving good reflections, ranging from 30° 58′ to 31° 26′, also gives 31° 12′. The ρ angle for D ($\bar{1}01$), with e as (110), is then 31° 12′, and the angle c (001) $\wedge$ D ($\bar{1}01$) in this position becomes (31° 12′+18° 52′) 50° 04′. In the orientation finally chosen, with e as (011), the faces c and a are interchanged, so that the angle 50° 04′ becomes that of D ($\bar{1}01$) $\wedge$ a (100), and ρ D ($\bar{1}01$) in the correct position is (90° 00′ − 50° 04′) 39° 56′.

With the values for β and the c axis already determined, the a axis is readily calculated from the ρ value (39° 56′) of D ($\bar{1}01$) and found to be 1.5230.

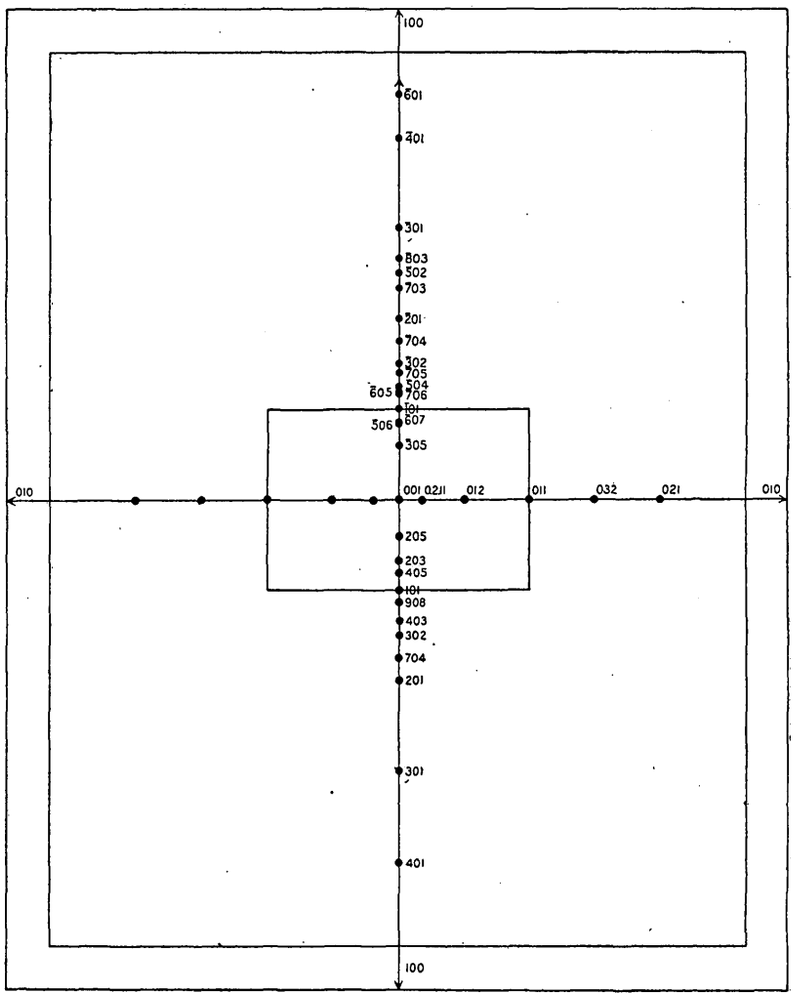

FIGURE 34.—Gnomonic projection of crystal forms of kernite

The axial elements for kernite then are $a : b : c$ = 1.5230 : 1 : 1.6989, β = 71° 08′, p'_0 = 1.1788, q'_0 = 1.6989, e' = 0.3417.

FORMS AND ANGLES

A total of 36 forms were determined to be present on the kernite crystals and fragments measured. These forms include the 3 pinacoids, 5 clinodomes, 11 positive orthodomes, and 17 negative orthodomes. Only forms belonging to the two dome zones are present, there being no prisms and no pyramids. The distribution of the forms is well shown in the gnomonic projection in Figure 34. Each of the forms was observed on at least two crystals. The forms

determined, with their average measured and calculated angles are shown in the table below.

Forms and angles of kernite

Form		Measured				Calculated			
Letter	Symbol	ϕ		ρ		ϕ		ρ	
		°	′	°	′	°	′	°	′
c	001	90	00	18	52	90	00	18	52
b	010	0	13	90	18	0	00	90	00
a	100	90	00	90	00	90	00	90	00
f	0. 2. 11	See table of measurements below.				47	53	24	44
g	012					21	55	42	29
e	011					11	22	59	57
h	032					7	38	68	45
i	021					5	45	73	41
j	205	90	00	38	49	90	00	39	07
k	203	90	00	47	52	90	00	48	26
l	405	90	00	52	01	90	00	52	06
d	101	90	00	56	35	90	00	56	40
n	908	90	00	59	04	90	00	59	03
p	403	90	00	61	52	90	00	62	24
q	302	90	00	64	20	90	00	64	38
r	704	90	00	67	19	90	00	67	25
s	201	90	00	69	45	90	00	69	40
t	301	90	00	74	23	90	00	75	32
u	401	90	00	77	56	90	00	78	49
A	$\bar{3}05$	90	00	20	08	90	00	20	05
B	$\bar{5}06$	90	00	32	47	90	00	32	39
C	$\bar{6}07$	90	00	33	42	90	00	33	46
D	$\bar{1}01$	90	00	39	56	90	00	39	56
E	$\bar{7}06$	90	00	45	52	90	00	45	57
F	$\bar{6}05$	90	00	47	10	90	00	47	01
G	$\bar{5}04$	90	00	48	38	90	00	48	32
H	$\bar{7}05$	90	00	52	28	90	00	52	37
J	$\bar{3}02$	90	00	54	49	90	00	54	58
K	$\bar{7}04$	90	00	59	46	90	00	59	51
L	$\bar{2}01$	90	00	63	36	90	00	63	37
M	$\bar{7}03$	90	00	67	35	90	00	67	27
N	$\bar{5}02$	90	00	69	02	90	00	69	00
P	$\bar{8}03$	90	00	70	23	90	00	70	21
Q	$\bar{3}01$	90	00	72	29	90	00	72	37
R	$\bar{4}01$	90	00	76	56	90	00	77	07
S	$\bar{6}01$	90	00	81	49	90	00	81	33

As the clinodomes were measured in the orientation where they functioned as prisms, their true ϕ and ρ values were not measured; instead, the angle c (001)$\wedge okl$ was measured. These measurements are shown in the table below, in which the numbers of the crystals are given at the left of the individual measurements. The values in parentheses are given as a matter of record; they are not used in obtaining the average values. Measurements of *e* (011) are given on page 152.

Measurements of clinodomes, kernite

[Angle = (001)$\wedge$(*okl*)]

	f (0.2.11)	*g* (012)	*h* (032)	*i* (021)
	° ′	° ′	° ′	° ′
Calculated	16 18	38 48	67 29	72 43
Average of measurements	16 26	38 47	67 32	72 18
Individual measurements	15—16 19	8—38 03	9—67 20	8—72 03
	16—16 25	10—(36 15)	14—67 44	9—72 33
	17—16 33	15—39 23		12—(70 28)
		17—38 44		
		18—38 56		

DESCRIPTION OF FORMS

The combinations observed on the 20 fragments measured are shown in the following table. The fragments 8 and 9, 11 and 12, 13 and 14, and 16, 17, and 18, belonging respectively to the same crystal, are grouped together, the letter of the crystal being repeated for each fragment on which it was determined. Fragments 1 to 12 are simply small cleavage pieces which happened to show faces other than the cleavages. Nothing is known as to the combination of the crystal from which they were cleaved. The measurements on the cleavage fragments had been made before the embedded complete crystals were found. Similarly, fragments 13 and 14 and fragments 16, 17, and 18 are, respectively, only part of the whole crystal. In removing the embedded crystals from the kernite matrix, parts of crystals 13 and 16 remained attached to the matrix, and other small pieces were lost. So the comparison of the relative abundance of the different crystal forms, as given below, is based only on five crystals, Nos. 13, 15, 16, 19, and 20, and is necessarily incomplete.

The two pinacoids *c* and *a*, the clinodome *e*, and the negative unit orthodome *D* are the only forms present on all five crystals. Five other forms occur on four of the crystals—namely, the positive orthodome *d* and the negative orthodomes *B*, *E*, *G*, *H*. A single form, *i* (021), was not found on any of the last five crystals, and three other forms, *h* (032), *k* (203), and *l* (405), were present on only one of the five crystals. All the other forms occurred on two or three of these crystals.

Combinations observed on measured fragments and crystals of kernite

Letter	Symbol	1	2	3	4	5	6	7	8, 9	10	11, 12	13, 14	15	16, 17, 18	19	20
c	001	As cleavage faces										*c c*	*c*	*c c c*	*c*	*c*
a	100											*a a*	*a*	*a a a*	*a*	*a*
b	010	.	.	.	.	.	.	.	*b b*	*b*	. .	. .	.	*b . b*	.	.
f	0. 2. 11	.	.	.	.	.	.	.	. .	.	. .	. .	*f*	*f f .*	.	.
g	012	.	.	.	.	.	.	.	*g .	*g*	. .	. .	*g*	*. g g*	.	.
e	011	.	.	.	.	.	.	.	*e e*	*e*	*e e*	*e e*	*e*	*e e e*	*e*	*e*
h	032	.	.	.	.	.	.	.	*. h*	.	. .	*. h*	.	. . .	.	.
i	021	.	.	.	.	.	.	.	*i i*	.	. *i*	. .	.	. . .	.	.
j	205	.	.	.	.	.	.	.	. .	.	. .	. .	.	*j j .*	.	*j*
k	203	.	.	.	*k*	.	*k*	.	. .	.	. .	. .	.	. . .	.	*k*
l	405	.	.	.	.	.	.	.	*l* .	.	. .	*l* .	.	. . .	.	.
d	101	.	.	.	*d*	.	.	.	. .	.	. .	*. d*	*d*	*d d .*	.	*d*
n	908	.	.	.	.	.	.	.	. .	.	. .	*n n*	.	. . .	.	*n*
p	403	.	.	.	.	.	.	.	. .	.	. .	*p p*	.	. . .	.	*p*
q	302	.	.	.	.	.	.	.	. .	.	. .	. .	.	*q q q*	.	*q*

Combinations observed on measured fragments and crystals of kernite—Continued

Letter	Symbol	1	2	3	4	5	6	7	8, 9	10	11, 12	13, 14	15	16, 17, 18	19	20
r	704	.	.	.	.	.	.	.	. .	.	. .	*r r*	*r*	. . .	.	.
s	201	.	.	.	.	.	.	.	. .	.	. .	. .	*s*	*s s* .	.	.
t	301	.	.	.	.	.	.	.	. .	.	. .	*t t*	.	*t* . .	.	.
u	401	.	.	.	*u*	.	.	.	. .	.	. .	*u* .	.	. . .	.	*u*
A	305	*A*	.	.	.	.	.	*A*	. .	.	. .	*A A*	.	. *A A*	.	.
B	506	.	*B*	.	.	.	.	.	. .	.	. .	*B* .	*B*	. . .	*B*	*B*
C	607	.	.	.	.	.	.	.	. .	.	. .	. .	*C*	. . .	.	*C*
D	101	*D*	*D*	*D*	.	*D*	.	*D*	*D D*	*D*	*D D*	*D D*	*D*	. . *D*	*D*	*D*
E	706	*E*	.	.	.	.	*E*	.	. .	.	. .	*E* .	*E*	. . .	*E*	*E*
F	605	.	.	.	.	.	.	.	. .	.	. .	. .	*F*	. . .	*F*	*F*
G	504	.	*G*	.	*G*	.	.	.	. .	.	. .	. *G*	*G*	. . .	*G*	*G*
H	705	.	.	.	.	.	*H*	.	. .	.	. .	. .	*H*	*H* . .	*H*	*H*
J	302	.	.	.	.	.	.	.	. .	.	. .	. .	.	. . .	*J*	*J*
K	704	.	.	.	.	.	.	.	*K* .	.	. .	. .	*K*	*K* . .	*K*	.
L	201	*L*	*L*	*L*	*L*	.	.	.	. *L*	.	. .	. .	*L*	. . .	.	*L*
M	703	.	.	.	.	.	.	.	*M* .	.	. .	. .	.	. . .	*M*	*M*
N	502	.	.	.	.	.	.	.	. .	.	. .	. .	.	. . .	*N*	*N*
P	803	.	.	.	.	.	.	.	. .	.	. .	. .	*P*	. . .	*P*	*P*
Q	301	.	.	.	.	.	.	.	. .	.	. .	. .	*Q*	. . .	*Q*	.
R	401	*R*	.	.	.	.	*R*	.	. .	.	. .	. .	*R*	. . .	*R*	*R*
S	601	.	*S*	.	.	.	.	.	*S* .	.	. .	*S* .	*S*	. . .	.	*S*

The orthopinacoid *a* (100) is probably the largest form on any of the crystals, though *e* (011) and *D* (101) are on some crystals nearly as large. It varies considerably in size and on some crystals is little more than a series of repeated broad striae or line faces, forming with the other faces of the orthodome zone a continuous set of rounded faces, heavily striated horizontally. A few of the large faces of *a* are not heavily striated, but usually where there is a set of rounded and striated domes running together the beginning of the striae can be seen on the faces of the orthopinacoid.

The clinopinacoid *b* (010) is a very insignificant form for the crystals measured, although it may possibly reach a large development on some of the large crystals embedded in the clay matrix. On all its observed occurrences it was a line face, between the two faces of the clinodome *e* (011) and gave poor reflections. The measurements are as follows:

Measurements of b (010) kernite

Crystal No.	Measured ϕ (calculated 0° 00′)	Measured ρ (calculated 90° 00′)
	° ′	° ′
8	−0 35	90 01
9	−2 38	90 00
10	−0 35	90 00
16	+2 11	91 10
18	+0 32	90 18

The basal pinacoid *c* (001) is a medium-sized form, usually several times as long as wide, with the direction of elongation at right angles for the upper and lower faces. It is usually striated parallel to the orthodomes but nevertheless is smooth and brilliant, affording the best reflection of all the forms. The excellent cleavage naturally likewise affords perfect reflections.

The unit clinodome *e* (011) belongs, with *a* (100), to the largest and dominant forms of kernite. If many complete crystals were available for observation, it might be found that *e* (011) was the largest form. The faces of *e* have a tendency to be slightly uneven and to lack the high luster of the natural faces of *a* and *c*. The form is at places slightly striated parallel to its intersection with *c* (001). Rather characteristically, it gives two reflections, with a difference as great as half a degree, one of them generally being better and brighter than the other.

The other clinodomes are represented only by long, narrow faces—broad line faces—giving distinct but poor reflections. The angles measured have already been given. The form system in the zone *c* (001) $\wedge$ *b* (010) is simple, except for the form *f* (0.2.11), which was noted on one crystal (No. 15) and two fragments (Nos. 16 and 17) of another crystal (No. 16). The consistent measured angles are close to the calculated angle and considerably apart from the calculated values for (015) = 17° 49′ (001$\wedge$*okl*) and for (016) = 15° 00′.

The positive orthodomes are characteristically very narrow faces, practically line faces, giving poor but distinct reflections. Only a very few of the faces are any broader than line faces. As a group they are not as large or common as the negative orthodomes. The measurements of all the faces of the positive orthodomes are presented in the table below, in which the numbers of the crystals are given at the left of the individual measurements.

Measurements of ρ angle of positive orthodomes, kernite

	j (205)	*k* (203)	*l* (405)	*d* (101)
	° ′	° ′	° ′	° ′
Calculated	39 07	48 26	52 06	56 46
Average of measurements	38 49	47 52	52 01	56 35
Individual measurements	16—39 27	4—48 12	8—51 46	4—(54 39)
	17—38 53	6—47 29	13—52 16	14—57 05
	20—38 07	20—47 54		15—56 28
				15—56 20
				16—56 40
				16—(57 54)
				17—56 24
				20—(58 10)

Measurements of ρ angle of positive orthodomes, kernite—Con.

	n (908)	*p* (403)	*q* (302)	*r* (704)
	° ′	° ′	° ′	° ′
Calculated	59 03	62 24	64 38	67 25
Average of measurements	59 04	61 52	64 20	67 19
Individual measurements	13—59 03	13—61 19	16—63 29	13—67 39
	14—59 06	14—62 11	17—63 29	14—67 22
	20—59 04	20—61 48	18—65 27	15—66 56
		20—62 12	20—64 56	

	s (201)	*t* (301)	*u* (401)
	° ′	° ′	° ′
Calculated	69 40	75 32	78 49
Average of measurements	69 45	74 23	77 56
Individual measurements	15—70 28	13—75 06	4—77 21
	16—69 46	14—73 55	13—77 57
	17—69 02	16—74 07	20—78 29

The difference in prominence between the positive and negative orthodomes can perhaps be shown by the similar difference in the occurrence of the two unit forms. The positive dome *d* (101) is present on but 5 crystals, and only 6 faces were measured, whereas the negative dome *D* ($\bar{1}01$) occurred on 13 crystals and 16 faces were measured. Also the positive section of the orthodome zone did not contain the large number of vicinal forms which are present in the negative section of the zone.

In discussing the symbols of the positive domes, according to the well-known procedure of Goldschmidt in applying the law of complication, the zone, from *c* (001) to *a* (100), yields:

Form	*c*	*j*	*k*	*l*	*d*	*n*	*p*	*q*	*r*	*s*	*t*	*u*	*a*
Symbol	0	$\frac{2}{5}$	$\frac{2}{3}$	$\frac{4}{5}$	1	$\frac{9}{8}$	$\frac{4}{3}$	$\frac{3}{2}$	$\frac{7}{4}$	2	3	4	∞

Splitting the zone at 1 and considering the two parts separately, we have:

Form	*c*	*j*	*k*	*l*	*d*		*d*	*n*	*p*	*q*	*r*	*s*	*t*	*u*	*a*
Symbol	0	$\frac{2}{5}$	$\frac{2}{3}$	$\frac{4}{5}$	1		1	$\frac{9}{8}$	$\frac{4}{3}$	$\frac{3}{2}$	$\frac{7}{4}$	2	3	4	∞
$\frac{v}{1-v}$	0	$\frac{2}{3}$	2	4	∞		$v-1$	0	$\frac{1}{8}$	$\frac{1}{3}$	$\frac{1}{2}$	$\frac{3}{4}$	1	2	3	∞
$\frac{v}{2}$	0	$\left[\frac{1}{3}\right]$	1	2	∞		N_3	0	$\left(\frac{1}{8}\right)$	$\frac{1}{3}$	$\frac{1}{2}$	$\left[\frac{2}{3}\right]$	1.	2	3	∞
N_2	0	$\frac{1}{2}$	1.	2	∞											

The form *j* should have the symbol $\frac{1}{2}$ = (102) instead of $\frac{2}{5}$ = (205), in order to fit into the series N_2. However, the ρ angle for (102) is 42° 56′, a figure 4° different from the measurements. The zone simply shows slight disturbance caused by the (second) intersecting clinodome zone. In the second part of the zone, the form *n* (908), so close to *d* (101), is obviously extra. However, the measurements are so remarkably consistent and close to the calculated value that the form is accepted, especially as it occurs in addition to *d* (101) and does not simply replace that as a vicinal form. The form *r* gives $\frac{3}{4}$ instead of the $\frac{2}{3}$ of the normal series. This raises the question whether its symbol should not be (503), for which the ρ angle is 66° 32′. Two of the three measurements, however, agree so much better with the indices (704) that they are taken as correct for the form *r*, even though they are obviously more complex.

The only positive dome shown in any of the crystal drawings is *d* (101), which is shown as narrow faces in Figures 38 and 39 and, what is unusual, as a relatively broad face in Figure 35.

The negative orthodomes have, in general, a large effect in determining the general habit of the crystals. The negative dome *D* ($\bar{1}01$), either by itself or in conjunction with a series of forms of fairly complicated indices, makes up a large part of the surface of the crystals. The large face *D* is invariably striated and is very likely to show both convex and concave forms. Especially prone is it to repeat itself all over the crystal as minute striae and to develop a striated zone, which on the goniometer gives a continuous solid band of reflections. On other crystals, however, the set of faces accompanying *D* give sharp and separate reflections, which are easily and accurately measurable. The faces of *D* commonly alternate with those of *a* (100), as shown in Figures 36 and 37. The associated domes of more complex indices may be so abundant, large, and repeated as practically to displace the unit form. (See fig. 40.)

As shown in Figure 40, *D* may be replaced by other domes, here chiefly *P* and *K*, and this repeated alternation of fine line faces will constitute practically the whole front surface of a crystal. A similar occurrence of striated and alternating faces of *D* is shown in Figure 39.

Although most of the negative domes, like the positive ones, are very narrow faces, practically line faces, a few are much larger faces, or rather, perhaps, sets of faces, or sets of repeated alternating striae, such as are shown, for example, in Figure 36, where the large faces of *N* and *H* are sets of striae, most of which belong to *N* and *H*, or in Figure 40, where again the large faces of *K*, *P*, *N*, *H*, *E* are really a composite set of striae, composed predominantly of faces of the form shown. They will also form a set of fine lines, which give sharp and distinct reflections for each form, but in which the individual forms are hardly recognizable, as shown in Figure 38 for *P*, *Q*, *R*, *S*. On this crystal, for comparison, the faces of *K*, *H*, and *G* are broader and distinct, not verging nor repeated.

The measurements of the negative orthodomes, except for *D* ($\bar{1}01$), which have already been given,

are listed below. The numbers of the crystals are shown at the left of the individual measurements.

Measurements of ρ angle of negative orthodomes, kernite

	A ($\bar{3}05$)	B ($\bar{5}06$)	C ($\bar{6}07$)	E ($\bar{7}06$)
	° ′	° ′	° ′	° ′
Calculated	20 05	32 39	33 46	45 57
Average of measurements	20 08	32 47	33 42	45 52
Individual measurements	1—20 17	2—32 37	15—33 48	1—46 02
	7—20 34	13—32 06	20—33 36	6—46 07
	13—20 30	15—33 19		13—46 35
	14—20 02	19—33 11		15—45 43
	17—19 54	20—32 44		19—45 33
	18—19 32			20—45 14

	F ($\bar{6}05$)	G ($\bar{5}04$)	H ($\bar{7}05$)	J ($\bar{3}02$)
	° ′	° ′	° ′	° ′
Calculated	47 01	48 32	52 37	54 58
Average of measurements	47 10	48 38	52 28	54 49
Individual measurements	15—47 17	2—48 26	6—52 17	19—54 49
	19—47 14	4—48 33	15—52 15	20—54 48
	20—46 58	14—49 14	16—52 33	
		15—48 27	19—52 44	
		19—48 58	20—52 33	
		20—48 48		

Measurements of ρ angle of negative orthodomes, kernite—Contd.

	K ($\bar{7}04$)	L ($\bar{2}01$)	M ($\bar{7}03$)	N ($\bar{5}02$)
	° ′	° ′	° ′	° ′
Calculated	59 51	63 37	67 27	69 00
Average of measurements	59 46	63 27	67 35	69 02
Individual measurements	8—59 41	1—63 04	8—67 55	19—68 53
	15—60 23	2—63 38	19—67 25	20—69 11
	16—58 51	3—63 13	20—67 26	
	19—60 10	4—(64 28)		
		9—63 52		
		15—63 41		
		20—63 14		

	P ($\bar{8}03$)	Q ($\bar{3}01$)	R ($\bar{4}01$)	S ($\bar{6}01$)
	° ′	° ′	° ′	° ′
Calculated	70 21	72 37	77 07	81 33
Average of measurements	70 23	72 29	76 56	81 49
Individual measurements	15—70 12	15—72 32	1—76 24	2—82 24
	19—70 31	19—72 25	6—(78 42)	8—(83 01)
	20—70 27		15—77 29	13—81 25
			19—77 09	15—81 37
			20—76 41	20—(79 45)

The discussion of the negative domes follows, the gnomonic projection showing that a division can also be made at L ($\bar{2}01$):

Form	c	A	B	C	D	E	F	G	H	J	K	L	M	N	P	Q	R	S	a
Symbol	0	$\frac{3}{5}$	$\frac{5}{6}$	$\frac{6}{7}$	1	$\frac{7}{6}$	$\frac{6}{5}$	$\frac{5}{4}$	$\frac{7}{5}$	$\frac{3}{2}$	$\frac{7}{4}$	2	$\frac{7}{3}$	$\frac{5}{2}$	$\frac{8}{3}$	3	4	6	∞

$\frac{v}{1-v}=0$	$\frac{3}{2}$	5	6	∞	1	$\frac{7}{6}$	$\frac{6}{5}$	$\frac{5}{4}$	$\frac{7}{5}$	$\frac{3}{2}$	$\frac{7}{4}$	2	2	$\frac{7}{3}$	$\frac{5}{2}$	$\frac{8}{3}$	3	4	6	∞
$\frac{v}{3}=0$	$\frac{1}{2}$	$\frac{5}{3}$	2	∞	$v-1=0$	$\frac{1}{6}$	$\frac{1}{5}$	$\frac{1}{4}$	$\frac{2}{5}$	$\frac{1}{2}$	$\frac{3}{4}$	1	$v-2=0$	$\frac{1}{3}$	$\frac{1}{2}$	$\frac{2}{3}$	1	2	4	∞
$N_2=0$	$\frac{1}{2}$	[1]	2	∞	$\frac{v}{1-v}=0$	$\frac{1}{5}$	$\frac{1}{4}$	$\frac{1}{3}$	$\frac{2}{3}$	1	3	∞	$N_3=0$	$\frac{1}{3}$	$\frac{1}{2}$	$\frac{2}{3}$	1 . 2	[3]	∞	
					$N_3=0$	$\left(\frac{1}{5}\right)$	$\left(\frac{1}{4}\right)$	$\frac{1}{3}$. $\frac{2}{3}$		1 . . 3		∞								

The form B($\bar{5}06$) should be ($\bar{3}04$), yielding 1 in the normal series N_2. The ρ angle for ($\bar{3}04$) is 28° 29′, 4° different from the measurements. The two forms corresponding to $\frac{1}{5}$ and $\frac{1}{4}$, E and F, are both extra in the series agreeing with the normal series N_3. E was measured six times and F three times; the measured angles agree well with the calculated angle. The form S, to fit perfectly in the normal series N_3, should give 3 instead of 4. The value of 3 would correspond to a symbol of ($\bar{5}01$), the calculated ρ angle of which is 79° 47′. Although a single face on crystal 20 gave a reading agreeing within 2′ of this value, the face is nevertheless referred to ($\bar{6}01$), as the other measurements of this steepest dome all give higher values, and two of them agree well with the angle for ($\bar{6}01$).

It is difficult to show the extreme value of such a discussion of crystal forms without going into great detail, showing the results first obtained, discussing them, and then by comparison with the normal series trying out the better agreeing figures and thus finally correcting, if necessary, the indices first chosen. It must suffice here to state that the discussion has been, as it always is in crystallographic description, of the greatest value in correctly deciphering the proper indices for the various forms.

VICINAL FORMS

It is with considerable diffidence that a series of vicinal negative domes are here listed. The writer is in general opposed to the listing of vicinal forms with high indices. One of the chief reasons against their presentation here is that so few complete crystals were available that it can not be satisfactorily determined that they really are a salient feature of the crystallography of kernite. Three other considerations, however, have outweighed this objection. The first is that they are present on all the complete crystals measured (Nos. 15, 19, and 20). The second is the consistency of their angular measurements and the close agreement of the measured and calculated values. Compare for example, the set of measurements of the group of the last five vicinal forms, beginning with those for ($\bar{1}$7.0.6). Or compare the two measurements for ($\bar{1}$2.0.5) or the three measurements for ($\bar{1}$7.0.11) or for ($\bar{3}$1.0.23). The third reason for giving them is that they are nearly always present in addition to the form of simpler indices to which they are vicinal. On the goniometer their signals,

though faint and described as poor, are as good and definite as the signals for the accepted forms. In fact, during the measurements, no difference was noted between the signals for the faces later found to be vicinal and those which gave relatively simple indices. Moreover, the table of measurements of the negative domes (p. 156) and the list of combinations show that the accepted forms with very simple indices (not higher than the figures of normal series N_3), such as $(\bar{3}02)$ and $(\bar{3}01)$, are much rarer than those of semivicinal indices, such as $(\bar{3}05)$, $(\bar{3}06)$, $(\bar{7}06)$, and $(\bar{5}04)$. Also a number of indices belonging to the normal series N_3, such as $(\bar{1}03)$, $(\bar{1}02)$, and $(\bar{2}03)$, are missing. The greater number of negative domes lie between $D(\bar{1}01)$ and $a(100)$ and similarly, all the vicinal forms except one lie between $D(\bar{1}01)$ and $a(100)$. It does not simplify matters to change the position of the unit dome. Neither was any other orientation found that would simplify the indices, the general morphology of kernite, with the large dominant faces *a D e* and the two excellent cleavages *c* and *a*, being kept in mind.

Should an abundance of complete crystals of kernite be available sometime and carefully measured, a fuller understanding of the complex indices of the vicinal forms might be attained. For the present, the results obtained are presented as found. To one interested in theoretical questions they may serve as the basis of discussion.

The vicinal forms found, with their occurrence and angles, are given here. As in the preceding tables, the numbers of the crystals are shown at the left of the individual measurements.

Measurements of ρ angle of vicinal negative domes, kernite

	$(\bar{2}1.0.22)$	$(\bar{2}1.0.20)$	$(\bar{1}4.0.13)$	$(\bar{1}1.0.10)$
	° ′	° ′	° ′	° ′
Calculated	38 05	41 52	42 52	43 41
Average of measurements	38 03	41 49	42 48	43 48
Individual measurements	15—38 03	8—41 56	6—43 13	15—43 42
	20—38 03	15—41 39	15—42 47	16—44 17
		20—41 58	19—42 44	18—43 43
			20—42 26	20—44 00

	$(\bar{6}07)$	$(\bar{2}1.0.16)$	$(\bar{3}1.0.23)$	$(\bar{1}7.0.11)$
	° ′	° ′	° ′	° ′
Calculated	49 34	50 19	51 17	55 57
Average of measurements	49 32	50 20	51 17	56 00
Individual measurements	14—49 14	19—50 34	15—51 20	4—55 57
	19—49 46	20—50 23	19—51 17	19—56 08
	20—49 36		20—51 15	20—55 55

	$(\bar{1}3.0.8)$	$(\bar{2}7.0.13)$	$(\bar{1}3.0.6)$	$(\bar{1}2.0.5)$
	° ′	° ′	° ′	° ′
Calculated	57 34	64 36	65 41	68 06
Average of measurements	57 35	64 38	65 32	68 05
Individual measurements	2—58 07	4—64 28	19—65 39	19—68 08
	6—57 48	19—64 36	20—65 24	20—68 02
	15—57 15	20—64 49		
	19—57 32			
	20—57 11			

Measurements of ρ angle of vicinal negative domes, kernite—Con.

	$(\bar{1}7.0.6)$	$(\bar{3}4.0.11)$	$(\bar{2}3.0.7)$
	° ′	° ′	° ′
Calculated	71 33	73 09	74 11
Average of measurements	71 36	73 09	74 10
Individual measurements	2—71 57	15—73 23	19—74 03
	15—71 34	19—73 03	20—74 17
	18—71 13	20—73 01	
	19—71 44		
	20—71 32		

	$(\bar{1}7.0.5)$	$(\bar{2}9.0.8)$	$(\bar{1}5.0.4)$
	° ′	° ′	° ′
Calculated	74 45	75 44	76 13
Average of measurements	74 47	75 48	76 18
Individual measurements	1—74 37	15—75 52	1—76 24
	8—(75 13)	19—75 42	19—76 17
	9—74 52	20—75 50	20—76 13
	15—74 43		
	19—74 43		
	20—74 55		

The three complete crystals measured, Nos. 15, 19, and 20, showed most of these vicinal forms. They were carefully remeasured, with special attention to the many reflections yielded by the faces in the orthodome zone. Although parts of this zone were so rounded as to give simply a continuous band of reflected light, most of the zone gave poor but very distinct single reflections. These were abundant and close together and yet sufficiently distinct to give a single undistorted reflection for each one measured. In order to show what the measurements yielded, those for these three complete crystals are given below in their entirety. Only those readings that were similar for at least two crystals are considered at all. Where but a single angular value was obtained, it is given as a matter of record, but no attempt at interpretation is offered. All these measurements may become of importance when a large suite of kernite crystals are available for accurate measurements.

Measurements of ρ angles of all negative orthodomes on kernite crystals Nos. 15, 19, and 20

[Vicinal forms not lettered]

	No. 15	No. 19	No. 20	Occurrences on other crystals
	° ′	° ′	° ′	
B $(\bar{5}06)$	33 19	33 11	32 44	Nos. 2, 13.
C $(\bar{6}07)$	33 48		33 36	
			34 31	
	35 05			
			37 27	
$(\bar{2}1.0.22)$	38 03		38 03	
			39 26	
D $(\bar{1}01)$	39 56	39 52	39 52	
	40 40			
$(\bar{2}1.0.20)$	41 39		41 58	No. 8.
$(\bar{1}4.0.13)$	42 47	42 44	42 26	No. 6.
$(\bar{1}2.0.10)$	43 42		44 00	Nos. 16, 18.
	44 33			
E $(\bar{7}06)$	45 43	45 33	45 14	Nos. 1, 6, 13.
	46 23			
	46 33			
F $(\bar{6}05)$	47 17	47 14	46 58	

Measurements of ρ angles of all negative orthodomes on kernite crystals Nos. 15, 19, and 20—Continued

[Vicinal forms not lettered]

	No. 15		No. 19		No. 20		Occurrences on other crystals
	°	′	°	′	°	′	
G (5̄04)	48	27	48	58	48	48	Nos. 2, 4, 14.
(9̄07)			49	46	49	36	No. 14.
(21̄.0.16)			50	34	50	23	
(31̄.0.23)	51	20	51	17	51	15	
H (7̄05)	52	15	52	44	52	33	Nos. 6, 16.
J (3̄02)			54	49	54	48	
(17̄.0.11)			56	08	55	55	No. 4.
(13̄.0.8)	57	15	57	32	57	11	Nos. 2, 6.
K (7̄04)	60	23	60	10			Nos. 8, 16.
					61	06	
L (2̄01)	63	41			63	14	Nos. 1, 2, 3, 4, 9.
					64	18	
(27̄.0.13)			64	36	64	49	
			65	02			
(13̄.0.6)			65	39	65	24	
					66	18	
M (7̄03)			67	25	67	26	No. 8.
(12̄.0.5)			68	08	68	02	
					68	46	
N (5̄02)			68	53	69	11	
			69	24			
P (8̄03)	70	12	70	31	70	27	
(17̄.0.6)	71	34	71	44	71	32	Nos. 2, 18.
Q (3̄01)	72	32	72	25			
(34̄.0.11)	73	23	73	03	73	01	
					73	47	
(23̄.0.7)			74	03	74	17	
(17̄.0.5)	74	43	74	43	74	55	Nos. 1, 8, 9.
(29̄.0.8)	75	52	75	42	75	50	
					76	13	
			76	44			
R (4̄01)	77	29	77	09	76	41	Nos. 1, 6.
					77	51	
					79	17	
	80	10					
S (6̄01)	81	37			79	45	Nos. 2, 8, 13.

DESCRIPTION OF CRYSTALS

All the measured crystals have essentially the same habit, varying only in detail on account of the large development of one crystal form at the expense of other forms. The crystals range from equidimensional ones to those which are slightly elongated in the vertical direction. The large development of the dome faces gives some of the crystals a wedge-shaped appearance. Rarely a set of repeated faces furnishes a rounded striated surface of relatively large extent which causes the crystal to be somewhat flattened.

The simple combinations *c, a, e; c, D, e; c, a, D, e,* which furnish the key habit of the kernite crystals and which the large crystals in the mine commonly show, are given in Figures 29, 30, and 31. In Figures 35 to 40 the attempt has been made to illustrate the general appearance of the crystals, giving only the dominant forms with but a few modifications, rather than to portray accurately the true appearance of the crystal, with all its faces and striations and distortions. Narrow striae of some of the forms are repeated on the crystals many more times than are shown in the drawings. Many rounded concave and convex surfaces, covered by such striated faces, are present, but only a few are shown. The two sides of the same crystal are not developed with the same forms or with equal development of the face of the same form, so that the appearance of the two sides of the same crystal may show considerable difference. The drawings are in part idealized, together with such distortion as seems to be characteristic of the kernite crystals.

In Figures 29 to 32 and 35 to 40 the guide line and angle point *W* have been somewhat shifted from the conventional standard position. In the standard position the face *e′* (0$\bar{1}$1) lies back of the guide line and would not show in the upper portion of the clinographic projection. The guide line consequently has been shifted up on the left side of the gnomonic projection a distance equal to that of *e′* (0$\bar{1}$1) from the standard position, so that *e′* (0$\bar{1}$1) lies midway between the standard and the shifted guide line. Moreover, the guide line has been shifted down on the right side of the projection so that it passes through the center of the projection. Several trials were made with the guide line in various positions, and the one finally adopted seems to illustrate best the appearance of the crystals in clinographic projection.

The more complicated crystals are developed as a crystallographic composite from the simple types and combinations shown in Figures 29, 30, and 31. Thus Figure 35, of which crystal 16 is an example, is a distorted modification of Figure 29. The top base is much broader than the bottom base, a feature not rare for kernite, and the direction of greatest length lies at right angles for the two faces of this form. Crystal 16 shows a broad face of *d* (101) and the largest face of *b* (010) observed on all the crystals. Figure 36 is a modification of the simple type of combination *c, a, e* (shown in fig. 29), where the front face of *a* (100) contains many occurrences of the negative domes, appearing repeatedly. In the center is a large concave area formed chiefly of *N* (5̄02) but containing additional negative domes not shown in the drawing. One side of crystal 20 shows such a development. The other side of crystal 20 (fig. 37) shows a similar development of forms, except that here the dome *D* (1̄01) is the prominent form, *a* (100) being very much diminished in importance, though the essential forms are *D* and *a*, with the negative domes, except the unit one, of very minor importance. This side of crystal 20 therefore represents a modification of the simpler type *c, D, e,* shown in Figure 30.

A modification of the simple type *c, a, D, e* (fig. 31) is represented by crystal 15, the two sides of which are shown in Figures 38 and 39. In Figure 38 the two faces of *e* (011) are drawn in symmetrical development. It is rather rare to find them so nearly equal in size. In Figure 39, showing the other side of crystal 15, the two faces of *e* (011) are drawn unequally developed, a condition that is rather common. In consequence

the two drawings do not accurately portray crystal 15 but are so drawn as to serve as types, illustrating the various modifications and distortions observed in the kernite crystals. Figure 38 shows the usual size of the faces of d (101), as does also Figure 39, and in addition the average size of the clinodomes other than e (011), here represented by g (012). In the center of a (100) is a concave striated hollow, bounded by faces of P ($\bar{8}03$), Q ($\bar{3}01$), R ($\bar{4}01$), S ($\bar{6}01$), often repeated. The center of the crystal shows the three faces of G ($\bar{5}04$), H ($\bar{7}05$), and K ($\bar{7}04$). Figure 39 has the simple form D ($\bar{1}01$) replaced in its upper portion by repeated alternations of striated faces of L ($\bar{2}01$) and D ($\bar{1}01$), together with other forms, and also shows broader faces of E ($\bar{7}06$), F ($\bar{6}05$), G ($\bar{5}04$), H ($\bar{7}05$), and J ($\bar{3}02$). The true representation of these repeated and striated faces would entail much more work than is justified.

Crystal 19 is represented by Figure 40, where the upper half of the front surface is composed largely of the orthopinacoid a (100), with small repeated striae

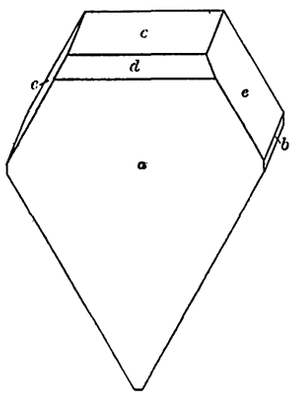

FIGURE 35.—Kernite crystal 16. Modification of the simple type c, a, e, with unusually broad face of d (101) and the largest face of b (010) observed. The two faces of c (001) are unequally developed. The actual crystal is about 5 millimeters high

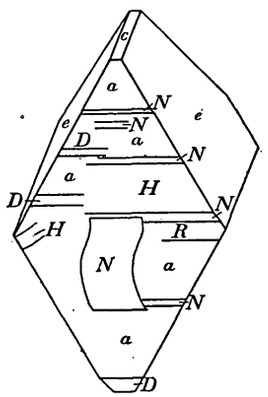

FIGURE 36.—One side of kernite crystal 20. Another modification of the simple type c, a, e, with many negative domes appearing repeatedly as broad and narrow striations and with a large concave face of N ($\bar{5}02$) accompanied by other negative domes not shown in the drawing. H ($\bar{7}05$), N ($\bar{5}02$), R ($\bar{4}01$)

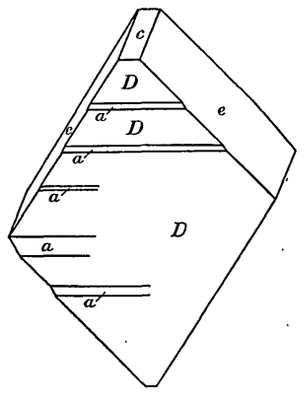

FIGURE 37.—The other side of kernite crystal 20, showing a modification of the type c, D, e, with alternations of a (100) and many negative domes, most of which occur as narrow faces on striations and are not shown in the drawing. Crystal 20, the two sides of which are shown in a simplified manner in Figures 36 and 37, is about 3 millimeters high

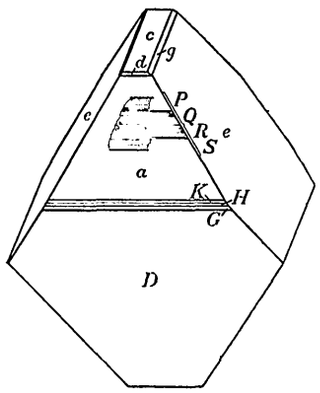

FIGURE 38.—One side of kernite crystal 15, showing the general type and only the more prominent negative domes P ($\bar{8}03$), Q ($\bar{3}01$), R ($\bar{4}01$), S ($\bar{6}01$), K ($\bar{7}04$), H ($\bar{7}05$), G ($\bar{5}04$). Other forms are d (101), g (012). The two faces of e (011) are drawn in ideal symmetry, a condition not often encountered

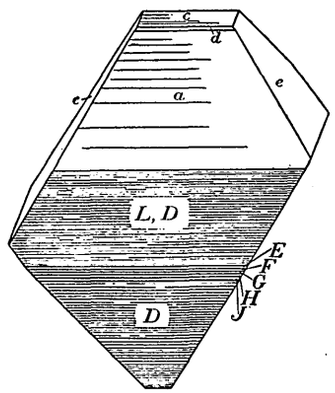

FIGURE 39.—The other side of kernite crystal 15, with the two faces of e (011) in unequal development, a more common condition than the symmetrical arrangement of Figure 38. The two drawings represent types of form development rather than a strict copy of the crystal measured. The unit positive dome d (101) is shown, with a striated orthopinacoid. The lower portion is a repeated combination of D ($\bar{1}01$) and L ($\bar{2}01$), with the broader faces of E ($\bar{7}06$), F ($\bar{6}05$), G ($\bar{5}04$), H ($\bar{7}05$), and J ($\bar{3}02$). The lower portion is again essentially D ($\bar{1}01$). Both these figures again show the change in position of greatest elongation of the two faces of the basal pinacoid c (001). Crystal 15 is about 2 millimeters high

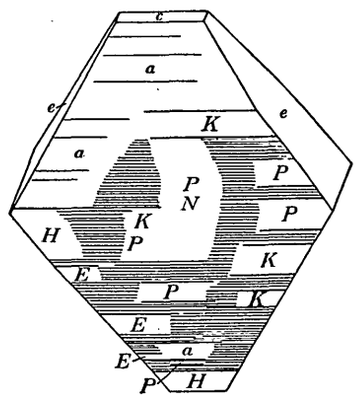

FIGURE 40.—One side of kernite crystal 19, with relatively large faces of K ($\bar{7}04$), P ($\bar{8}03$), N ($\bar{5}02$), H ($\bar{7}05$), and E ($\bar{7}06$). Although these faces are not striated in the drawing, actually they are finely striated and merge into the more coarsely striated parts, as shown in the drawing, where the individual faces can not be identified. Crystal 19 is about 2½ millimeters high

of some of the negative domes. The lower portion is a heavily striated composite of negative domes, some of which are represented by relatively broad faces.

TWINNING

None of the complete crystals measured showed any twinning, but on one of the larger compact masses there were groups of built-up individuals at about 60° that strongly suggested twinning. A large group of kernite, about 2 feet long, collected for exhibition in the National Museum, shows several such twin structures, and measurements of their angle and etching of the faces show that they are twinned with *e* (011) as the twinning plane. Measurement of their relative position gave a value of 61°, corresponding to the angle *c* (001) : *e* (011) of 58° 07′. The two faces of *a* (100) remain in the same plane; the two

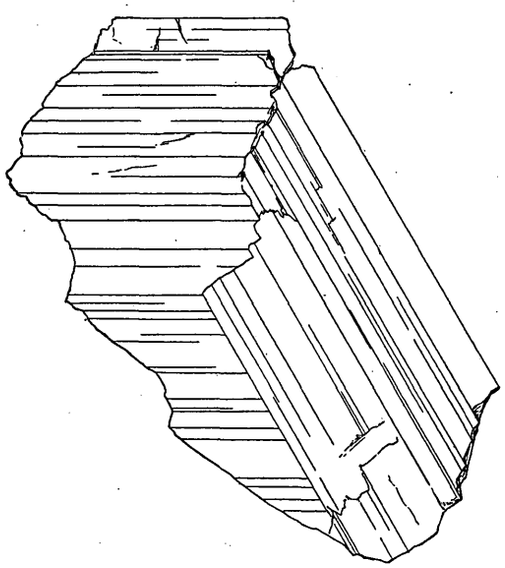

FIGURE 41.—Sketch of twin of kernite

faces of *c* (001) lie in the clinodome zone of the untwinned crystal. Figure 41 is a sketch of the appearance of such a twin grouping.

ETCHING EFFECTS

The two perfect cleavages of kernite easily develop characteristic etch figures, which show that the cleavages do not belong to the same crystal form. The etchings also serve admirably for the identification of the cleavages. These etchings were called to the writer's attention by Dr. C. Hlawatsch, of Vienna, who said that they showed that kernite could not be orthorhombic in symmetry, as stated in the preliminary report.

After several modifications of treatment had been tried out, it was found that excellent etchings could be obtained if a cleavage fragment of kernite was immersed in hot water for about 10 seconds. Longer treatment covers the entire surface with etchings which run together and are not as distinct. In fact, a cleavage fragment of kernite appears to become dull white when left in water, either hot or cold, for some time, owing to the multiplicity of the etchings. Hot water is the most practicable liquid to use if the etchings are developed for purposes of orientation of the cleavage fragment and are desired quickly. Cold water gives just as good results, but the etchings are developed much more slowly. When immersed in cold water, the etch figures are large enough to differentiate in about 5 minutes, and a 10-minute immersion suffices to develop them to a satisfactory size, so that their shape and symmetry can be seen.

In general, the etchings on the basal pinacoid *c* (001) are square in outline, and those on the orthopinacoid *a* (100) are triangular, pointing upward. The basal pinacoidal cleavage also shows the fine parting lines, normal to the edge (001) ∧ (100), as described in connection with cleavage. Although groups of etchings on both faces can be seen to run in all directions,

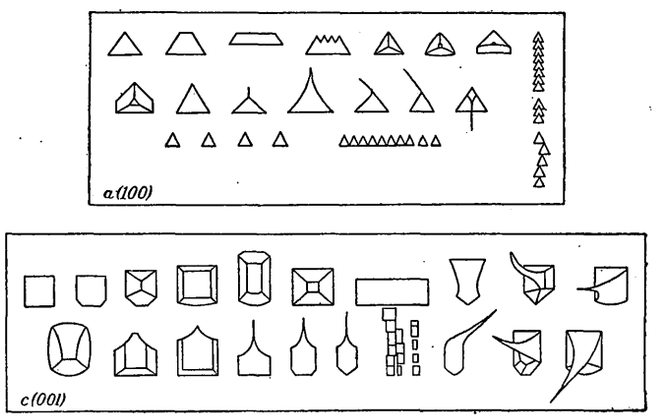

FIGURE 42.—Etch figures artificially developed on the cleavage surfaces of *c* (001) and *a* (100) of kernite, by immersion in hot water for 10 seconds. On the left side are shown the more simple types

there is a tendency for those on the basal pinacoid to form chains normal to the edge (001) ∧ (100), whereas the chains of etchings developed on the front pinacoid *a* (100) have a general tendency to run parallel to the intersection edge (001) ∧ (100).

All the etch figures, free from beaks, have a plane of symmetry parallel to *b* (010) and clearly indicate monoclinic symmetry. Many of the square etchings on the base *c* (001) have their base more modified than their top, so that there clearly is no horizontal plane of symmetry to them. The various types observed, which were not specially studied, are shown in Figure 42.

Not a few of the etch figures have developed considerable beaks, which, though in general vertical, run in all directions, as shown particularly on the right side of the lower sketch of Figure 42. The writer had no opportunity of making any detailed study of these etchings, but the ease with which the etchings can be obtained renders kernite excellent material for such a study.

If a very dilute acid is used, or even if a drop or two of dilute acid is added to the water in which the kernite is immersed, the shape of the etching on *c* (001) is changed from a square outline to long, thin ovals, of a not very definite shape, with rather characteristic small and very short beaks growing out of the middle on each of the sides. The general appearance of these etch figures as developed by dilute HCl is shown in Figure 43. With very dilute H_2SO_4, similar figures were obtained, but the ovals were somewhat broader.

The very dilute acid solution produces triangular etchings on *a* (100) similar to those produced by water, except that the sides of the triangle are rounded instead of being straight. Horizontal chains are very characteristic. The appearance of these etchings is shown in Figure 43.

Etch figures are just as readily obtained on the other surfaces of kernite. Cleavage plates after *D* ($\bar{1}01$), a third cleavage of fair quality, on immersion in hot water for 10 seconds, develop etch figures resembling a flaring gas jet. The surface of this

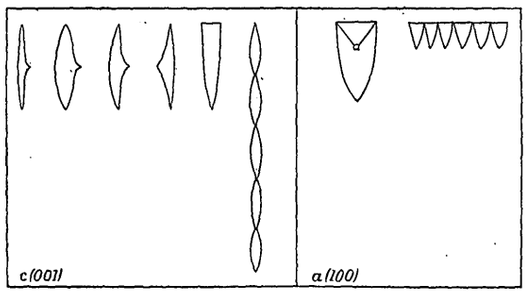

FIGURE 43.—Etch figures artificially developed on cleavage faces of kernite by immersion in very dilute acid

cleavage is not as plane as those of the cleavages *a* (100) and *c* (001), and the etchings are not as distinct. They also clearly show only the vertical plane of symmetry, parallel to *b* (010). The general appearance of these etchings is shown in Figure 44.

On fracture surfaces parallel to the clinopinacoid *b* (010) hot water produces etch figures similar to those shown in Figure 44. This surface, being parallel to the plane of symmetry, develops etchings of a different symmetry than the cleavages in the orthodome zone (normal to the clinopinacoid), but their symmetry belongs to the monoclinic system. All the observed etchings indicate monoclinic symmetry for kernite, and nothing was seen to suggest definitely any deviation from holohedral symmetry.

Kernite contains many planes, both straight and curved, in which lie an abundance of liquid inclusions and negative crystals. Some of these are sharply angular, and others appear considerably rounded. The general direction of elongation of the negative crystals follows the *b* axis, but some are at right angles to it, and others extend in diverse directions.

CHEMICAL PROPERTIES

PYROGNOSTICS

Kernite readily fuses before the blowpipe flame, with expansion, to an opaque white cauliflower mass. On further heating, it fuses to a clear glass (borax glass). When heated in a closed tube, it expands, curls up, cleaving into numerous fibers, and expands considerably more to a large white mass, finally condensing and fusing to clear borax glass. It is slowly soluble in cold water, a clear piece appearing dull white in a short time, owing to the formation of innumerable etch figures on the surface. A piece 1 centimeter long and half as thick will not be completely dissolved on standing in cold water over night. Kernite is readily soluble in hot water and in acids. The solution, on evaporation of the water, yields 1.39 times as much borax.

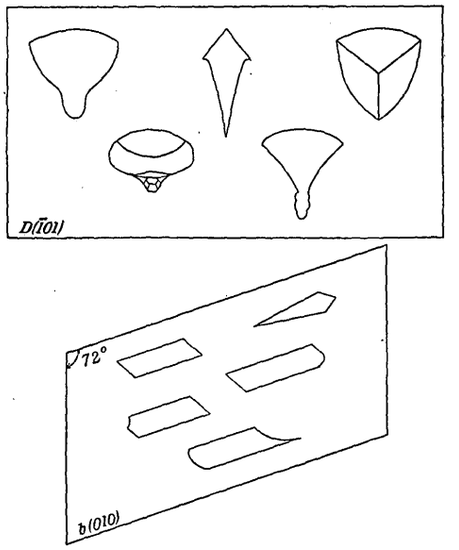

FIGURE 44.—Etch figures on kernite artificially developed on the cleavage surface parallel to *D* ($\bar{1}01$) and on the clinopinacoid *b* (010). Produced by immersion in hot water for 10 seconds

ANALYSIS

The chemical composition is as follows:

Analysis of kernite

[W. T. Schaller, analyst]

	Analysis	Calculated	Artificial
Na_2O	22. 63	22. 66	22. 65
B_2O_3	50. 76	51. 02	[a] 50. 80
H_2O	26. 50	26. 32	26. 55
	99. 89	100. 00	100. 00

[a] By difference.

The ratios of the analysis of kernite are $Na_2O : B_2O_3 : H_2O = 365 : 729 : 1{,}472$, or $1.00 : 1.99 : 4.02$, giving the formula $Na_2O.2B_2O_3.4H_2O$, or $H_8Na_2B_4O_{11}$. Nearly half the total water is given off up to 110°, and only three-quarters of the total water is lost up to 200°,

there being no swelling of the mineral at this temperature. The water lost at different temperatures is:

Water lost on heating kernite

	Per cent	Per cent of total
Up to 110°	10. 88	41
From 110° to 200°	9. 08	34
At ignition (above 200°)	6. 45	25
	26. 41	100

Of the water lost at 110°, 82 per cent was reabsorbed in balance case in 1½ days.

ALTERATION

Kernite that is free from any other borate (borax, for example) and that has been kept in the laboratory for nearly two years, exposed to the air, is perfectly stable, no cloudiness being developed. But if any borax (and possibly other borates) is attached to the kernite, it partly alters to opaque white tincalconite in a few months. The progress of the alteration can readily be observed in crushed fragments under the microscope. The tincalconite coats the kernite and also develops in cleavage cracks, gradually replacing the kernite. Several clear pieces of kernite show the development of small rounded areas of tincalconite along a cleavage plane in the interior of the kernite. The change of kernite ($Na_2O.2B_2O_3.4H_2O$) to tincalconite ($Na_2O.2B_2O_3.5H_2O$) consists chemically simply in the addition of one molecule of water. This change, however, is mechanically very destructive, for a large specimen of kernite, 2 feet long, fresh and solid when collected, is in less than a year splitting to pieces, owing to the development of tincalconite along its cleavage planes.

SYNTHESIS

Many futile attempts were made to prepare kernite artificially from borax. Fusions of borax in open and closed tubes, with the expulsion of part of the water, invariably yielded only the 5-hydrate, artificial tincalconite. Crystallization in the presence of various other salts, of which a long list was tried, yielded no success. Very gradual evaporation of a solution of borax near 100° yielded only fine crystals of the 5-hydrate. R. C. Wells, of the Geological Survey laboratory, became interested in the problem and finally succeeded in making a preparation from borax that yielded almost pure artificial kernite, only a few crystals of artificial tincalconite being associated with it.

The method used was to heat borax in a closed tube to about 150° for several days in an electric furnace, the outside end of the tube being bent down so that the water driven off from the borax was condensed and collected here and did not return to the heated borax. Under these conditions, the heating was continued for several days; the furnace was cooled, and then the water driven off was allowed to flow back onto the heated borax, the furnace reheated, and the tube again introduced and kept at 150° for several days. When cooled and examined, the resultant product was all crystalline and consisted essentially of small kernite crystals with only a very small quantity of the 5-hydrate. The optics and the chemical composition of the artificial product, as already given, agree with that of kernite.

The small crystals, averaging between a fifth and a tenth of a millimeter in size, have the appearance shown in Figure 45, being considerably more elongated in the direction of the *b* axis than the natural crystals. The faces of *a* (100) and *c* (001) are the dominant ones, with those of *e* (011) the only essential terminal ones. Faces of *d* (101), *D* ($\bar{1}01$), and *f* (0.2.11) are present

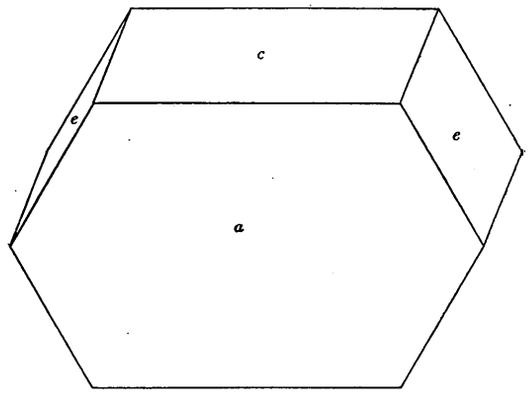

FIGURE 45.—Crystal of artificial kernite, about a fifth of a millimeter long

as line faces, and broader faces of the pyramid (322), between *a* and *e*, were noted on several crystals. It is curious that the artificial crystals should show pyramid faces, totally lacking on the natural crystals. The measurements on the artificial crystals yielded the following angles:

Measurements on artificial crystals of kernite

Angle	Measured		Calculated	
	°	′	°	′
c (001) ∧ *a* (100)	71	15	71	08
c (001) ∧ *e* (011)	57	57	58	07
c (001) ∧ *f* (0.2.11)	16	30	16	18
a (100) ∧ *e* (011)	80	16	80	10
c (001) ∧ *d* (101)	37	40	37	48
c (001) ∧ *D* ($\bar{1}01$)	58	49	58	48
a (100) ∧ (322)	43	01	43	04

An earlier experiment, made by Mr. Wells under similar conditions, except that the water driven off was not allowed to run back on the heated borax, yielded a crystalline product whose analysis showed it to be the 3-hydrate.

Analysis of artificial 3-hydrate

[W. T. Schaller, analyst]

	Analysis	Ratio	Calculated
Na_2O	23. 16	0.95 or 1	24. 88
B_2O_3	[a]55. 64	2.03 or 2	58. 86
H_2O	21. 20	3.03 or 3	19. 26
	100. 00		100. 00

[a] By difference.

The sample analyzed was not completely crystallized, small particles of an amorphous material being intermingled. The optical properties (both β and γ being higher than 1.50) showed that no kernite or higher hydrate was present.

The bearing of the success attained in making artificial kernite is discussed under heading "Origin of deposit."

TINCALCONITE

OCCURRENCE

The name tincalconite was given by Shephard [10] to a pulverulent and efflorescent borax from California, containing 32 per cent of water. Although no further description is given, it is obvious that his material was the 5-hydrate of the borax series, $Na_2O.2B_2O_3.5H_2O$ identical in composition with "octahedral borax." A sample of Shephard's original tincalconite, now in the United States National Museum, is identical with the tincalconite from the Kramer district.

Tincalconite was found, not very abundant but rather widespread, coating both borax and kernite. As it forms readily from the 10-hydrate, or borax, by partial dehydration, it probably occurs at many places in the Mohave Desert of southern California and can probably be found as a coating on many of the borax deposits of the desert region. Microscopic examination of these films and included cleavage fragments of kernite definitely shows the order of formation, the tincalconite being later than and derived from the kernite. Tincalconite derived from and coating borax did not seem to be nearly as abundant in the mine, although the dull-white film was seen at a few places in the mine coating some of the massive borax. In the Washington laboratory the samples of borax quickly dehydrate to tincalconite, the glassy borax becoming covered with a dull-white layer in a few months. The appearance of tincalconite as it develops naturally in the Washington laboratory from borax is well illustrated in Plate 25, *B*. The kernite, too, if any borax is present, readily alters to tincalconite in the laboratory.

Tincalconite is the natural equivalent of what has long been known as "octahedral borax." This 5-hydrate crystallizes in the hexagonal-rhombohedral system, but the combination of six rhombohedra and two bases greatly resembles an octahedron, and hence this compound has been (wrongly) called octahedral borax. The *c* axis was determined by Arzrumi on artificial crystals to be 1.87. The forms are *c* (0001), *r* ($10\bar{1}1$), *d* ($01\bar{1}2$). No natural crystals of tincalconite were observed.

PHYSICAL AND OPTICAL PROPERTIES

The natural material was very unsuitable for determination of its properties, as it occurs only as a fine-grained crystalline powder. In appearance it is dull white, although artificial crystals are vitreous in luster, colorless, and transparent. The artificial crystals show no cleavage on breaking but a hackly fracture with an occasionally poorly developed conchoidal surface. The specific gravity of the artificial crystals was determined as 1.880. This is considerably higher than that given in the literature (1.815), which was determined by Payen [11] over a hundred years ago!

The artificial crystals of tincalconite are uniaxial positive, $\omega = 1.461$, $\epsilon = 1.474$, $B = 0.013$. These values are the average of three determinations as follows:

Indices of artificial tincalconite

	Schaller		Ross	Average
	1927	1928		
ω	1. 460	1. 462	1. 461	1. 461
ϵ	1. 473	1. 476	1. 474	1. 474

The mean index $\frac{(2\omega + \epsilon)}{3}$ is 1.465. The natural mineral is so fine grained that accurate determination of refractive indices is difficult. The mean index was measured on one sample as 1.463, and Shephard's original material gave the same value.

CHEMICAL COMPOSITION

PYROGNOSTICS

The pyrognostics of artificial tincalconite are similar to those of other members of the borax group.

ANALYSIS

A number of samples of tincalconite were analyzed. Of these, only the two (Nos. 1 and 2) that coat kernite were collected as such in the mine. The other three samples have developed in the Washington laboratory on borax.

Samples 1 and 2 coat kernite and were present on the kernite when collected, though it is possible that the alteration of kernite to tincalconite has continued after the specimens were brought to Washington. Sample 1 is a fine-grained crystalline mass, and the powder analyzed contained a very few minute fibers of kernite. Sample 2 was prepared from a single

[10] Shephard, C. U., Soc. Min. Bull., vol. 1, p. 144, 1878.

[11] Payen, A., Jour. chimie méd., vol. 3, p. 594, 1827.

cleavage piece of what was originally all kernite but had changed to tincalconite, a true pseudomorph, as the cleavage shape of the kernite was retained. This piece was crushed, and as much kernite as possible was removed, the remaining sample being the typical fine-grained crystalline powder so characteristic of this pseudomorphous tincalconite. Many of the minute cleavage fibers of kernite have been completely changed to tincalconite. The total quantity of kernite remaining in the sample analyzed was small, the impurities in the sample being determined as consisting of 1.32 per cent (of the original sample) of clay (ignited) and 2.11 per cent of kernite (not ignited). In the table below this analysis is given as made (2a) and repeated with the clay and kernite deducted (2b).

Sample 3 was a fine-grained crystalline mass of tincalconite coating massive borax and developed after the samples reached Washington. A very few small pieces of borax were contained in the sample analyzed.

Sample 4 was collected from seams in the clay matrix, associated with a little kernite. The seams, when collected, were probably borax, which changed to tincalconite in the Washington laboratory. The associated clay (insoluble in water) gave a loss on ignition of 11.85 per cent. The sample analyzed was very finely crystalline, with a few pieces of borax and a very few fibers of kernite. These associated minerals stand out strikingly in a slide of the analyzed powder of tincalconite, as the individual crystal units of kernite and of borax are very large in comparison to those of the fine-grained tincalconite. Several fibers of kernite completely altered to tincalconite are present. Much of the tincalconite is so fine grained as to appear almost opaque under low magnification.

Sample 5 is a borax crystal (natural or artificial?) from Searles Lake, Calif., naturally dehydrated in the Washington laboratory.

The samples analyzed gave no reaction for any appreciable lime, magnesia, sulphate, chloride, or carbonate.

Analyses of tincalconite from California

[W. T. Schaller, analyst]

	1	2a	2b	3	4	5	Calculated
Insoluble in cold water	0.48	3.43	------	0.37	0.90	0.25	------
Na_2O	20.80	19.97	20.67	21.28	20.72	21.40	21.29
B_2O_3	47.52	47.00	48.67	47.26	47.19	47.26	47.80
H_2O (total)	30.59	29.75	30.81	30.78	30.93	31.01	30.91
	99.39	100.15	100.15	99.69	99.74	99.92	100.00

As can readily be seen, the analyses of tincalconite agree closely with the calculated composition. The ratios are as follows:

Ratios determined from analyses of tincalconite

	1	2b	3	4	5
Na_2O	0.99	0.97	1.01	0.99	1.01
B_2O_3	2.01	2.03	1.99	2.01	1.99
H_2O	5.01	4.98	5.02	5.09	5.05

The analyses and the resultant ratios clearly show that the formula of tincalconite is $Na_2O.2B_2O_3.5H_2O$.

The loss of water on a sample of artificial tincalconite is as follows:

Water lost on heating artificial tincalconite

	Per cent	Per cent of total
Up to 110°	16.03	50
From 110° to 200°	10.82	34
At ignition	5.31	16
	32.16	100

There was no reabsorption of the water lost up to 110° on letting the sample stand in the balance case over night.

SYNTHESIS

Tincalconite can readily be made by boiling a solution of borax until crystallization ensues or by letting a hot strong solution cool to not below 60°. Crystals of tincalconite also readily form by melting borax in its water of crystallization, in either a closed or an open tube. Tincalconite represents the stable form of $Na_2O.2B_2O_3.nH_2O$ above 60° or above about 35° in saturated salt solutions.

BORAX

The borax of the deposit does not show many features of strictly mineralogic interest. It is, however, of the greatest importance in considering the origin of the deposit of borate minerals.

Most of the borax associated with the kernite is massive, showing no crystal outline. (See pl. 26, *A*.) Several bodies of such massive borax, as large as an ordinary room, or even larger, were encountered. In appearance the massive borax resembles some massive greasy quartz or even more the massive compact elaeolite.

Included in the massive borax are a few imperfect and distorted crystals of kernite, spherulitic groups of kramerite, and sharply angular fragments of the clay matrix abundantly intersected and cut by minute veins of borax, which either run across the clay fragments or only partly cut into them. One specimen contained minute shredlike realgar, giving

the borax specimen an orange-colored mottled appearance. More rarely the borax is developed as porphyritic crystals, a centimeter or two long, in the clay matrix, as shown in Plate 26, *B*. The borax readily dehydrates to white opaque tincalconite in the laboratory.

The optical properties of this borax, so far as determined, show no difference from those already determined. The refractive indices of borax given in the literature show close agreement, as follows:

Refractive indices of borax

	α	β	γ
Dufet	1. 4467	1. 4694	1. 4724
Descloizeaux	1. 447	1. 470	1. 473
Tschermak	1. 4468	1. 4686	1. 4715
Kohlrausch	1. 4463	1. 4682	1. 4712
Average	1. 4467 1. 447	1. 4691 1. 469	1. 4720 1. 472

The borax from the Kramer district gave similar indices ($\alpha=1.446$, $\beta=1.468$, $\gamma=1.472$). A rather striking diagnostic property of borax, as observed under the microscope, is that sections normal to an optic axis pass through characteristic pinchbeck-brown to blue-gray colors instead of extinguishing.

ASSOCIATED MINERALS

The minerals, aside from other borates, associated with the borates above described are very few in number. They are, as determined, the clay minerals, calcite, realgar, and stibnite. The clay minerals comprise those of the clay itself and the associated rock minerals resulting from the disintegration of various rocks. The clay matrix, as the host of the kernite has been called, is a complex unit, of diverse origins. There are streaks and bands of hard clay in the softer material (such as are shown in pl. 25, *A*) and coarse and fine material, all aggregated together into the clay matrix. Several thin sections of different varieties of the clay matrix suggest that most of the clay mineral is beidellite.[12] One thin section shows uniform areas of fine-grained material, mixed with agglomeratic material, some of which suggest original porphyritic lava, with well-defined flow lines, and others suggest débris from granitic rocks, as for example the fragments of microcline and black tourmaline. Feldspars and micas, are abundant in parts of the clay. Considerable opaque black material (carbonaceous?) is irregularly scattered throughout the clay, as is also more or less calcite.

[12] For a description of the clay minerals, see Ross, C. S., and Shannon, E. V., The minerals of bentonite and related clays and their physical properties: Am. Ceramic Soc. Jour., vol. 9, pp. 77–96, 1926.

The clay carrying the seams of ulexite (pl. 22, *A*) lying above the kernite is far more homogeneous. It is much finer grained and resembles beidellite. The matrix of the colemanite-ulexite specimen (pl. 22, *B*) obtained above the kernite is coarser grained and resembles the clay of the kernite matrix. In spots there is abundant biotite, somewhat altered. Some of the clay resembles in structure the basalt lying below the colemanite-ulexite in the Suckow shafts, several miles to the west, especially in what seems to be a retention of the trachytic structure.

The calcite occurs in small aggregates of rhombohedral crystals and also as small masses of no definite shape scattered through the coarser clay, especially where this has the appearance of having been drived from an altered volcanic rock. The realgar was observed inclosed in one specimen of borax as fine shreds, giving the borax a mottled orange-colored appearance. A mass of cleavable realgar with a coarse radiating columnar structure, about half a centimeter across, was also observed in the clay associated with the black-appearing kernite. When heated in a glass tube, the realgar readily sublimed and partly oxidized to white arsenious oxide, which condensed as transparent, colorless, isotropic octahedra. Stibnite occurs characteristically as small spherulites, 1 millimeter or less in diameter, in the clay and in the borate minerals. It is present in greatest quantity in the specimens showing the radiating kramerite, and although in places it is concentrated so that a square centimeter of surface may show two or three spherulites, its total quantity in the deposit is very small. Most specimens show no sulphide mineral whatever.

ORIGIN OF DEPOSIT

In discussing the origin of the borate minerals of the Kramer district, one is greatly handicapped by the lack of quantitative knowledge of the geologic conditions. These have been described for the deposit just west of the kernite by Noble. For the Suckow shaft No. 2, in sec. 22, and probably the surrounding ones, the geologic formations comprise essentially an overlying alluvium (Quaternary), about 100 feet thick, which rests unconformably on the eroded surface of the upturned edges of the Tertiary sedimentary rocks. These, beginning at the top, consist of 75 feet of pale-greenish clay shale, somewhat sandy and containing volcanic ash, followed by 40 feet of an arkose sandstone with volcanic ash, which in turn is underlain by about 60 feet of the borate-bearing clay shale. Below this is lava, at least 20 feet thick. The borate-bearing clay shale with nodules of colemanite irregularly distributed through it, is everywhere mashed,

broken, and slickensided—a condition similar to that of the clay matrix of the kernite 2 miles to the east.

Noble considers that the contact of the borate shale and the lava is a depositional contact, the lava being a flow upon which the shale was deposited. The reported vesicular character of the top of the lava is adduced as evidence that it was a surface flow. In none of the shafts in the immediate vicinity of the Suckow shafts was any kernite or borax reported.

The colemanite and ulexite bearing clay of the Suckow shafts is probably similar to the clay carrying the same minerals which overlies the kernite. It is possible that the kernite-carrying clay is of the same formation, only thicker. Possibly this increased thickness is only local, and the kernite deposit may be the site of a former depression filled with a borax lake upon which the ulexite and colemanite bearing clays were deposited. Igneous rock is reported to underlie the kernite, just as lava underlies the other borate minerals in the Suckow shaft.

The discussion of the origin of the kernite deposit is based on a number of features, which first will be mentioned briefly and then treated at greater length. The general theory of the formation of the kernite here proposed is the one suggested by Mr. Thomas Cramer, chief chemist of the Pacific Coast Borax Co., at Wilmington, Calif. It is essentially that the kernite has formed by the fusion, chiefly in its own water of crystallization, of a preexisting accumulation of borax. The excess of water given off, permeating the overlying clay beds, may have dissolved the ulexite present, very likely as "cotton balls," and recrystallized it into the satinlike fibrous veins, a specimen of which is shown in Plate 22, *A*.

The features characterizing this deposit which may have had a decided influence in the formation of kernite are as follows:

1. No other deposit of kernite is known, so that the assemblage of conditions was probably very unusual.
2. Kernite is absent in the western part of the field.
3. The difficulty of artificially making kernite shows that the conditions of its formation are limited.
4. Large bodies of massive borax are present.
5. Small veins of borax cut the kernite.
6. Kernite crystals are embedded in massive borax.
7. Igneous rock underlies the deposit.
8. Stibnite and realgar are present.
9. Calcium borates are scarce.
10. Ulexite veins occur above the deposit.

These features are considered to be of importance with reference to the origin of the kernite deposit and are discussed below.

1. The fact the kernite is a new mineral, never before found and not made artificially, even though the borax-water system has been studied in the laboratory, indicates that it is the result of a combination of unusual conditions. Were it a common product, easily made artificially, it would have been found in many localities, especially in the borate regions of California and Nevada. Apparently no single item of the conditions would yield kernite naturally, but the combination of several such unusual conditions as existed in this region has produced enormous quantities of this most interesting and valuable mineral. One can not help wondering what other unusual mineral associations lie buried in other parts of the Mohave Desert.

2. The absence of kernite in the western part of the Kramer district, where both ulexite and colemanite are present in abundance, suggests that an additional factor to those favoring the formation of ulexite and colemanite must have been present. The same conditions that yield these two calcium borates would not yield kernite, and it is considered doubtful if there is any genetic relation between kernite and ulexite. The concentration of the kernite in the eastern part of the field suggests also that this side of the field had a different topographic expression, and that there was at one time a depression here wherein was concentrated sodium borate, probably only as borax, long before the overlying clay containing ulexite was laid down. A detailed topographic map, with plottings of the logs of all the shafts and drill holes of the region, would be needed before a definite conclusion could be reached regarding the existence of a depression in the eastern part of the field.

3. The difficulty of making kernite artificially shows that the conditions usually existing in natural regions containing borates would not suffice to produce kernite. The experiment of Wells, in which the 3-hydrate was obtained at 150°–160° by heating borax in a closed tube, shows that the upper limit of stability of the 4-hydrate kernite lies near 150°–160°. The continuous production of the 5-hydrate by boiling a solution of borax and also by melting borax in its water of crystallization in both open and closed tubes, and the experiments of the writer in duplicating Wells's experiment but obtaining only the 5-hydrate, all suggest that the upper limit of stability of the 5-hydrate and consequently the lower limit of stability of the 4-hydrate is considerably above 100° and very likely not much below 150°. This leaves a very narrow range of stability for the 4-hydrate. Wells's success in obtaining kernite artificially by allowing the water distilled off to flow back on the sodium borate and reheating and redistilling off part of the water shows that pressure and the presence of some excess water are probably needed for the formation of the 4-hydrate. If the kernite was formed by the fusion of the preexisting borax in its own water of crystallization, then the clay matrix probably acted as a retardant for the free and ready escape of all the excess water, and it may be that the presence of such excess water not only helped but was essential in the production of the 4-hydrate, just as in Wells's successful experiment.

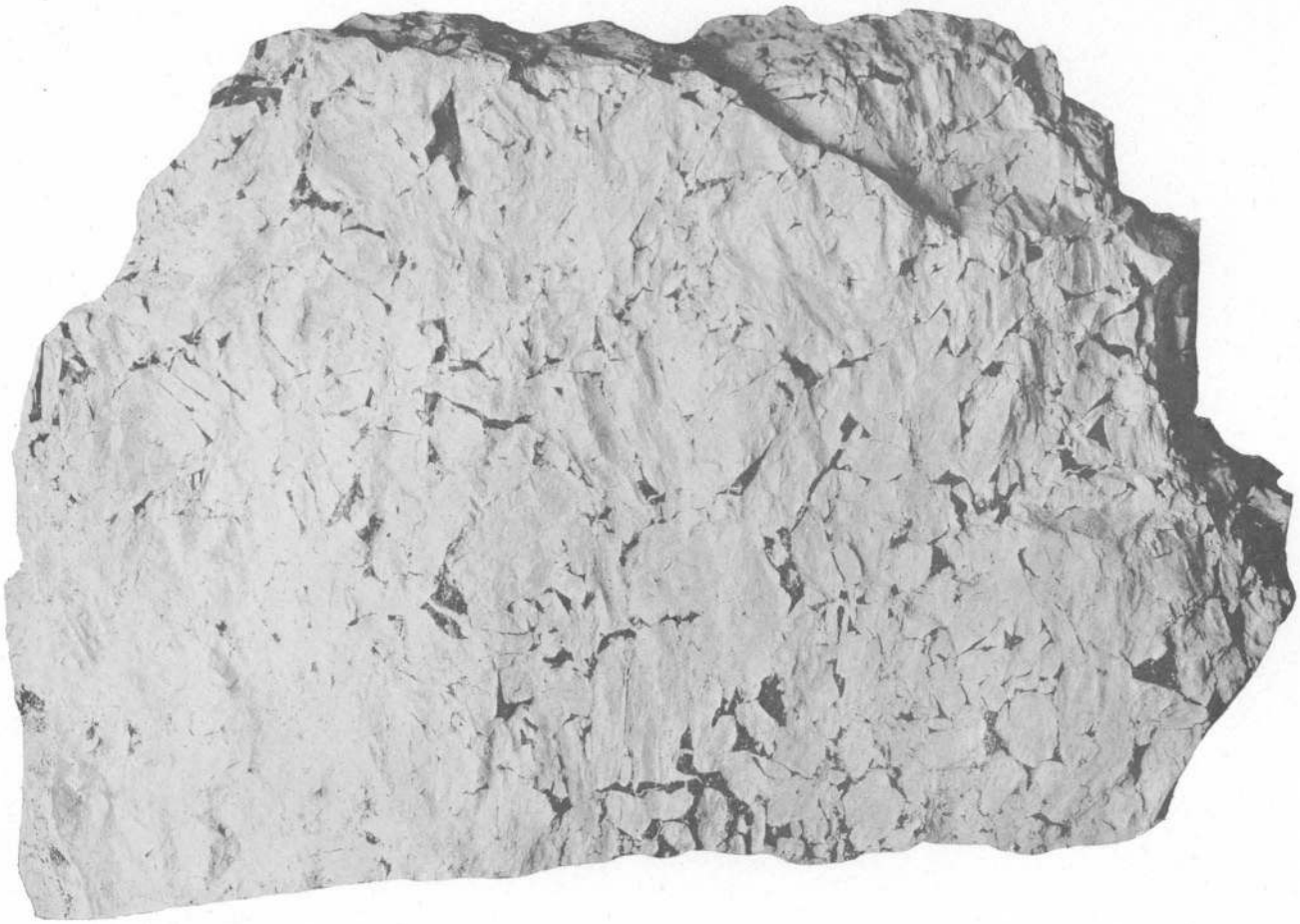

A. MASSIVE BORAX SUPERFICIALLY ALTERED TO TINCALCONITE

U. S. National Museum catalog No. 95838. Natural size.

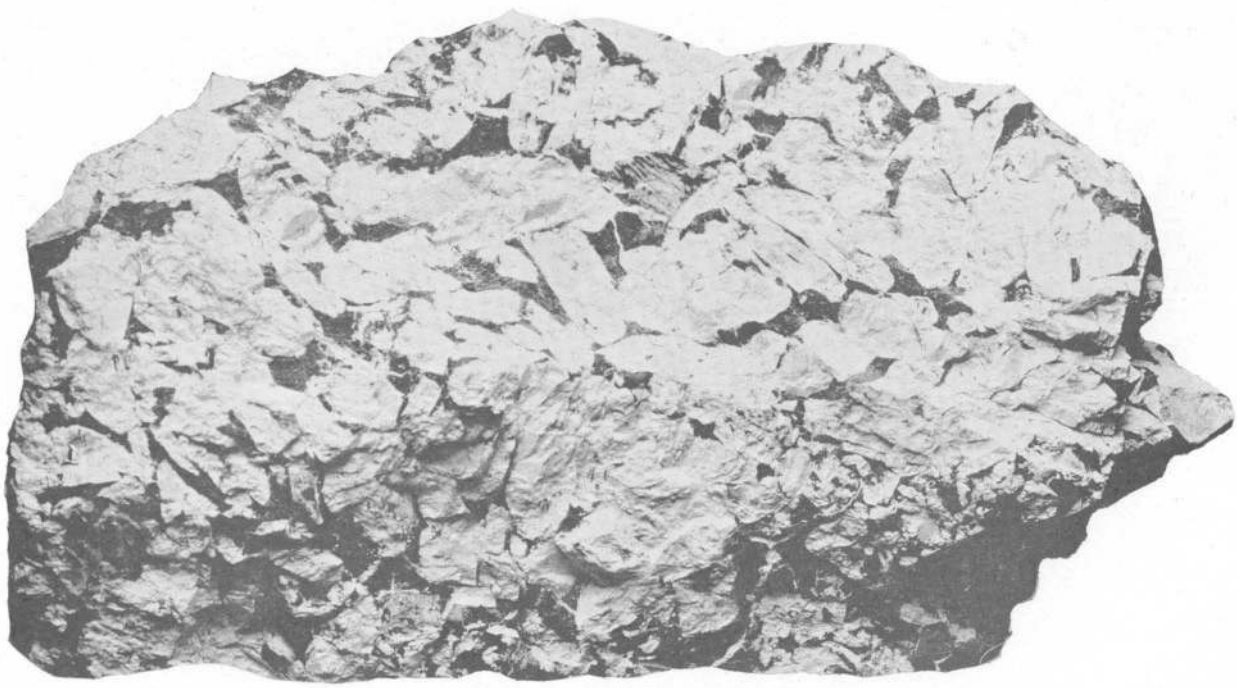

B. CRYSTALS OF BORAX IN CLAY SUPERFICIALLY ALTERED TO TINCALCONITE

U. S. National Museum catalog No. 95839. Natural size.

BORAX AND TINCALCONITE

A. LARGER KERNITE CRYSTALS BETWEEN LAYERS OF SHALE

B. AGGREGATE OF LARGE KERNITE CRYSTALS

OCCURRENCE OF KERNITE IN THE BAKER DEPOSIT, PACIFIC COAST BORAX CO., KRAMER DISTRICT, CALIFORNIA

Photographs by W. F. Foshag, U. S. National Museum. One-fifteenth natural size.

4. The presence of large bodies of massive borax, such as are illustrated in Plate 26, *A*, indicates the form that an aggregate of borax crystals, when fused, would take, provided the escape of any water was prevented by an impervious surrounding clay. These large bodies of massive borax, showing practically no crystal outline, are not the form taken by borax crystallizing out of solution. It seems therefore that the assumption is justified that at one time large quantities of borax existed here in a molten state. If the escape of all water was prevented, only massive borax would result on cooling; if some water escaped, a lower hydrate would have to form; and if conditions were just right and the necessary quantity of water escaped, then kernite might readily form. The clay with the porphyritic crystals of borax, as shown in Plate 26, *B*, a rather rare occurrence, might represent the original borax crystals embedded in the clay or, more probably, a recrystallization of the massive borax into distinct crystals. The nonuniformity of the clay, with the presence of harder (and more impervious?) layers, as shown in Plate 25, *A*, strongly supports the idea that in parts of the deposit the escape of any water from any molten borax might well have been hindered.

5. The small veins of massive borax, apparently cutting kernite (pl. 25, *A*), may be a later effect, though they may be only apparent veins and actually may represent residua of the fused borax from which no water could escape.

6. The kernite crystals embedded in massive borax offer one of the most interesting associations for speculation about their origin. If kernite was derived from the fusion and partial dehydration of borax—an assumption considered to represent the conditions but in no way proved—then the explanation of this association becomes simple. Parts of the fused borax lost enough water to permit the formation of kernite, which started to grow as a solid, the consequent loss of volume being readily taken up by the still fused borax, which later crystallized as such in a massive form where no further escape of water could take place.

7. If the underlying igneous rock was extrusive and the original borax lake was deposited on it after it cooled, then a source of heat to fuse the deposit must be looked for. If, on the other hand, the igneous rock was intrusive and later than the original borax lake, then it would be the source of the heat that melted the borax crystals, whose partial dehydration then yielded kernite.

8. The presence of stibnite and realgar strongly suggests the underlying igneous rock as a source, these minerals probably being formed in the fumarole stage, after the molten rock had cooled considerably. In the absence of any knowledge of the extrusive or intrusive character of the igneous rock, the possible effect it may have had on the development of kernite must remain an unknown factor.

9. The scarcity of any calcium borates directly associated with the kernite shows that neither colemanite nor ulexite is directly connected with the formation of kernite, for the lime borates represent a fixed product. For example, in the formation of colemanite from ulexite, the lime borate colemanite is the fixed end product. The borax of the original (theoretical) deposit may represent the washed-out sodium borate from ulexite altering to colemanite, but it is doubtful whether the possibly higher deposits of ulexite to the west were ever extensive enough to furnish sufficient sodium borate to yield the immense deposit of kernite, though they may well have contributed. The source of the supposed original borax represents no greater difficulty than the origin of the borax in any of the borax lakes in the arid Southwest.

10. The ulexite veins (pl. 22, *A*) in the clay above the kernite deposit are believed to be later in their formation than the original borax deposit that changed to kernite. It is possible that the water escaping during the supposed dehydration of the original borax deposit entered the overlying clay and recrystallized any "cotton ball" ulexite that may have been present into the satinlike fibrous veins now found.

The theory of the origin of the kernite, as expressed to the writer by Mr. Thomas Cramer, seems to offer the best explanation. It is essentially as follows: A borax lake formerly occupied the area of the Kramer borate district. By evaporation of the water, borax crystallized out. Borax crystals may have been concentrated at the east side by wind (as suggested by Mr. Cramer), or there may have been a local depression at the east side into which the concentrated borax solution flowed, leaving only a relatively minor quantity of borax at the west end (in the region of the Suckow shafts). This borax was covered by mud and clay, with probably layers of volcanic ash. On top of this borax-bearing clay was deposited additional clay, also containing borates, more probably ulexite. This clay bed would correspond to the borate clays of the west end of the district. On top is the borate-free valley fill (sand and gravel). Heat from some source—the igneous rock if intrusive—melted the buried borax deposit in its own water of crystallization, a temperature of about 150° being reached. Enough of the water was driven off so that on cooling the 4-hydrate crystallized as kernite. Locally, where the escape of water was prevented by impervious clay, the fused borax solidified into massive borax. The excess of water driven off from the fused borax entered the overlying ulexite-carrying clay and recrystallized the original "cotton ball" ulexite into the fibrous veins now found.

BORON MINERALS

The following list comprises all the known boron minerals, in part arranged in systematic groups.

WITHOUT WATER

Avogadrite. $KF.BF_3$. A little caesium may be present, $(K, Cs)F.BF_3$.

Jeremejevite. $Al_2O_3.B_2O_3$. The name is here given, as by Dana, in the German transliteration from the Russian; the correct English transliteration, according to the standard rules of the Library of Congress and the Royal Society, is eremeyevite. Eichwaldite is considered to be a dimorphous form of the same compound.

Rhodizite. $4(H, Na, K, Cs, Rb)_2O.4BeO.3Al_2O_3.6B_2O_3$.

Nordenskioeldite. $CaO.SnO_2.B_2O_3$.

Ludwigite. $4MgO.Fe_2O_3.B_2O_3$. Synonyms, collbranite, magnesioludwigite.

Vonsenite. $4FeO.Fe_2O_3.B_2O_3$.

Pinakiolite. $4(Mg, Mn)O.Mn_2O_3.B_2O_3$.

Boracite. $5MgO.MgCl_2.7B_2C_3$. Synonym, stassfurtite. Iron boracite contains a little iron.

Warwickite. $6MgO.FeO.2TiO_2.3B_2O_3$. Synonym, enceladite.

WITH WATER; WITHOUT SILICA

Sassolite. $B_2O_3.3H_2O$.

Larderellite. $(NH_4)_2O.4B_2O_3.4H_2O$.

Paternoite. $MgO.4B_2O_3.4H_2O$.

Kaliborite. $K_2O.4MgO.11B_2O_3.9H_2O$. Synonyms, hintzeite, heintzite.

Bechilite. $CaO.2B_2O_3.4H_2O(?)$. Synonym, borocalcite. The existence of this mineral is doubtful.

Kernite. $Na_2O.2B_2O_3.4H_2O$. Synonym, rasorite.

Tincalconite. $Na_2O.2B_2O_3.5H_2O$.

Borax. $Na_2O.2B_2O_3.10H_2O$. Synonym, tincal.

Kramerite. $Na_2O.2CaO.5B_2O_3.10H_2O$.

Ulexite. $Na_2O.2CaO.5B_2O_3.16H_2O$. Synonyms, boronatrocalcite, cryptomorphite, franklandite, and many others.

Colemanite. $2CaO.3B_2O_3.5H_2O$.

Meyerhofferite. $2CaO.3B_2O_3.7H_2O$.

Inyoite. $2CaO.3B_2O_3.13H_2O$.

Hydroboracite. $CaO.MgO.3B_2O_3.6H_2O$.

Priceite. $5CaO.6B_2O_3.9H_2O$ or $4CaO.5B_2O_3.7H_2O$. Synonym, pandermite.

Pinnoite. $MgO.B_2O_3.3H_2O$.

Szaibelyite. $2MgO.B_2O_3.H_2O$. Synonyms, boromagnesite, camsellite(?), and possibly ascharite, which has been regarded as containing only two-thirds molecule of H_2O.

Camsellite. $2MgO.B_2O_3H_2O$. Probably the same as szaibelyite. Camsellite from California is supposed to contain some silica.

Sussexite. $2(Mn,Mg)O.B_2O_3.H_2O$.

Ascharite. $2MgO.B_2O_3.\frac{2}{3}H_2O(?)$. According to Van't Hoff's work, ascharite has the same formula as szaibelyite. It needs restudy.

Hambergite. $4BeO.B_2O_3.H_2O$.

Fluoborite. $6MgO.B_2O_3.3((OH),F)$.

Luenebergite. $3MgO.B_2O_3.P_2O_5.8H_2O$.

Sulphoborite. $6MgO.2SO_2.2B_2O_3.9H_2O$.

Hulsite. $12FeO.2Fe_2O_3.SnO_2.3B_2O_3.2H_2O$. Paigeite differs in containing a smaller proportion of tin but may be essentially the same.

Cahnite. $4CaO.As_2O_5.B_2O_3.4H_2O$.

Lagonite is a mixture of sassolite and limonite.

WITH SILICA

The formulas of many of the borosilicates are complex and uncertain. The minerals are arranged below alphabetically and not in systematic groupings.

Axinite. $2Al_2O_3.2(Fe, Mn)O.4CaO.H_2O.B_2O_3.8SiO_2$.

Bakerite. $8CaO.6H_2O.5B_2O_3.6SiO_2(?)$.

Cappelenite. Ba, Y, H, B, Si, O.

Caryocerite. Th, Ce, La, Nd, Pr, Y, Ca, H, F, B, Si, O.

Danburite. $CaO.B_2O_3.2SiO_2$.

Datolite. $2CaO.H_2O.B_2O_3.2SiO_2$.

Dumortierite. $8Al_2O_3.H_2O.B_2O_3.6SiO_2$.

Grandidierite. $11(Al, Fe, B)_2O_3.7(Mg, Fe, Ca)O.2(H, Na, K)_2O.7SiO_2$.

Homilite. $2CaO.FeO.B_2O_3.2SiO_2$.

Howlite. $4CaO.5H_2O.5B_2O_3.2SiO_2$.

Hyalotekite. $16(Pb, Ba, Ca)O.F.2B_2O_3.24H_2O$.

Kornerupine. $8MgO.6(Al, B)_2O_3.7SiO_2(?)$.

Manandonite. $7Al_2O_3.2Li_2O.12H_2O.2B_2O_3.6SiO_2$.

Melanocerite. Ce, Nd, Pr, La, Y, Ca, H, F, B, Si, O.

Sapphirine. $5MgO.6(Al, B)_2O_3.2SiO_2(?)$.

Searlesite. $Na_2O.2H_2O.B_2O_3.4SiO_2$.

Serendibite. $3Al_2O_3.2CaO.4MgO.B_2O_3.4SiO_2$.

Tourmaline. Al, Mg, Fe, Mn, Ca, Na, K, Li, H, F, B, Si, O. A group name including several species.

Tritomite. Th, Ce, La, Nd, Pr, Y, Fe, Ca, H, F, B, Si, O.

Vesuvianite. Al, B, Fe, Ca, Mg, H, Si, O. The variety wiluite contains the largest percentage of boron (as much as 4.2 per cent) but other varieties, from widely separated localities, contain smaller amounts.

This list of boron minerals contains several series of hydrates of the same compound—the kernite-tincalconite-borax series, the colemanite-meyerhofferite-inyoite series, and the kramerite-ulexite series. Their properties being known, a comparative study may be made.

The sodium borate series will be first considered. Evidences of the existence of artificial hydrates of $Na_2O.2B_2O_3$, other than the 5-hydrate and 10-hydrate, in a well-defined crystalline phase were not found in the literature. Lescoeur [13] mentions literature references to the 2, 3–4, and 6 hydrates, but these show no data of value on which the existence of such hydrates could be based. The 3-hydrate and 4-hydrate, for example, was amorphous and prepared at 100°. The 6-hydrate found by Bechi [14] as an incrustation at Tuscany, Italy, gave on analysis a composition agreeing in water content with the 6-hydrate, but Bechi gives no description whatever regarding the physical state or homogeneity of the material. An explanation as a mixture of borax with a more or less dehydrated borax (tincalconite?) is more probable.

The anhydrous amorphous compound belonging to this series, with zero water content, the well-known "borax glass," was found to have a density of 2.36 (determinations given in the literature are 2.371, 2.373,

[13] Lescoeur, H., Annales chimie et phys., 7th ser., vol. 9, pp. 543–546, 1896.

[14] Bechi, C., Jahrb. Chemie, vol. 7, p. 867, 1854; abstract in Am. Jour. Sci., 2d ser., vol. 19, p. 120, 1855.

and 2.5, the last obviously in error). The refractive index was determined to be 1.513 (1.513 for glass obtained from kernite, 1.513 for glass obtained from artificial tincalconite, and 1.513–1.514 for glass obtained from artificial borax). The value 1.515 is given in the literature. From the values of the density (d) and mean refractive index (n) the specific refractive index of B_2O_3 can be calculated, using the formula $\frac{n-1}{d}=K=\frac{k_1p_1}{100}+\frac{k_2p_2}{100}+\frac{k_3p_3}{100}$, k_n being the specific refractive index for the radicle whose percentage in the particular substance is given by p_n. The same values for Na_2O (0.181) and for H_2O (0.34) are used, taken from Larsen's tabulation.[15]

The values for the series of sodium borates then are as follows:

Properties of sodium borates

	d	n	k (B_2O_3)
Isotropic borax glass, $Na_2O.2B_2O_3$	2. 36	1. 513	0. 217
Kernite, $Na_2O.2B_2O_3.4H_2O$	1. 91	1. 471	. 228
	1. 95	1. 471	. 218
Tincalconite,[a] $Na_2O.2B_2O_3.5H_2O$	1. 88	1. 465	. 217
Borax,[a] $Na_2O.2B_2O_3.10H_2O$	1. 72	1. 463	. 217

[a] Artificial.

Two values are given for kernite, depending on the gravity. A density of 1.91 was determined, whereas a density of 1.95 would give a more consistent value for k. It is possible that the multitude of inclusions and negative crystals present in kernite have a lowering effect on the density of the whole mass. On the other hand, the constant figure 0.217 obtained for $k(B_2O_3)$ from the other members of the series may be accidental. The effect of the varying figure for the density on the calculated value of k may be shown for borax, where the specific refractive value, as calculated, will vary about 0.004 for each 0.01 difference in the density as here shown. Using the value of 1.463 for n, we find that the value of $k(B_2O_3)$ in borax varies according to the density, as follows:

$d=1.70$ $k=0.2256$ } $\Delta=0.0044$
$d=1.71$ $k=0.2212$ }
$d=1.72$ $k=0.2169$ } $\Delta=0.0043$
$d=1.73$ $k=0.2127$ $\Delta=0.0042$

The rather constant value of the mean index for the three hydrates (the differences being but slightly greater than the error of determination) is very striking. The density decreases, fairly regularly, with the increase in water content. The density (1.815) given in the literature for the 5-hydrate (artificial tincalconite) gave a discordant value for k. The density was therefore redetermined (heavy solution, bromoform and carbon tetrachloride) and found to be 1.88. On looking through the literature, only this one determination of the density of the 5-hydrate could be found,[16] and this was published over a hundred years ago!

The calcium borates form a series of three minerals, as follows:

Properties of calcium borates

	d	n	k(B_2O_3)
Colemanite, $2CaO.3B_2O_3.5H_2O$	2. 423	1. 597	0. 217
Meyerhofferite, $2CaO.3B_2O_3.7H_2O$	2. 12	1. 532	. 211
Inyoite, $2CaO.3B_2O_3.13H_2O$	1. 875	1. 505	. 215

Apparently, the slightly discordant value of 0.211 for k for meyerhofferite suggests that the value given for its density is not quite accurate. In this series the variation in the mean index corresponds with the variation in the density. Why the mean index in the sodium borate series is so nearly constant is not known.

The sodium-calcium borate series comprises kramerite and ulexite:

Properties of sodium-calcium borates

	d	n	k (B_2O_3)
Kramerite, $Na_2O.2CaO.5B_2O_3.10H_2O$	2. 141	1. 528	0. 217
Ulexite, $Na_2O.2CaO.5B_2O_3.16H_2O$	1. 963	1. 506	. 213

The average value of k for B_2O_3, using the values for Na_2O, CaO, and H_2O as given by Larsen, is close to 0.216.

Although comparisons of crystallographic axes of different minerals may lead to unwarranted deductions, it is worth while to call attention to such similarities as exist. Thus, for example, the axial ratios of kramerite are close to those of borax, and by fractionally changing those of colemanite and kernite, a similarity can be shown for four of these borates, all monoclinic:

Colemanite	$\frac{4}{3}a:b:c=1.0357:1:0.5430$	$\beta=69°\ 53'$
Kernite	$\frac{2}{3}a:b:\frac{1}{3}c=1.0153:1:0.5663$	$\beta=71°\ 08'$
Borax	$a:b:c=1.0995:1:0.5632$	$\beta=73°\ 25'$
Kramerite	$a:b:c=1.1051:1:0.5237$	$\beta=72°\ 16'$

[15] Larsen, E. S., The microscopic determination of the nonopaque minerals: U S. Geol. Survey Bull. 679, p. 31, 1921.

[16] Payen, A., Jour. chimie méd., vol. 3, p. 594, 1827. Payen also gives 1.74 as the density of borax.

BIBLIOGRAPHY

Only a few papers on the Kramer district or on its minerals have been published. They are arranged below by years.

Gale, H. S., Borate deposits near Kramer, Calif.: Am. Inst. Min. and Met. Eng. Trans., vol. 73, pp. 449–463, 1926.

Noble, L. F., Borate deposits in the Kramer district, Kern County, Calif.: U. S. Geol. Survey Bull. 785, pp. 45–61, 1926.

Gale, H. S., A new borate mineral: Eng. and Min. Jour.-Press, vol. 123, p. 10, 1927.

Schaller, W. T., Kernite, a new sodium borate: Am. Mineralogist, vol. 12, pp. 24–25, 1927.

Palmer, L. A., Kernite or rasorite?: Eng. and Min. Jour.-Press, vol. 123, p. 494, 1927.

New source of borax found in California: Chem. and Met. Eng., vol. 34, p. 264, 1927.

Record borax deposit: Science News-Letter, Apr. 9, 1927, p. 229.

Palmer, L. A., Concerning rasorite: Eng. and Min. Jour.-Press, vol. 125, pp. 207–208, 1928.

California kernite deposit most important source of borax in the world: Eng. and Min. Jour.-Press, vol. 125, p. 551, 1928.

United States has monopoly in borax industry: Daily Science News Bull. (Science Service), No. 367, A, sheet 3, Apr. 2, 1928.

Gale, H. S., Naming the new borax mineral: Eng. and Min. Jour.-Press vol. 125, p. 702, 1928.